

# 锡钨锂矿化与外围脉状铅锌银铜矿化的内在成因 关系和形成机制

——以内蒙古维拉斯托锡钨锂多金属矿床为例<sup>\*</sup>

周振华, 高旭, 欧阳荷根, 刘军, 赵家齐

(中国地质科学院矿产资源研究所 自然资源部成矿作用与资源评价重点实验室, 北京 100037)

**摘要** 大兴安岭南段维拉斯托锡钨锂多金属矿是近年来新发现的大型矿床, 具有“上脉下体”的垂向矿化分带特征, 矿集区范围内表现出以花岗岩体为中心的高温锡钨钼矿化、中温铜锌矿化、外围低温铅锌银铜矿化的水平分带。目前, 对锡钨锂多金属矿化与外围脉状铅锌银铜矿化的内在成因关系和形成机制及深部地质背景还缺乏足够的认识。Ar-Ar年代学研究结果表明, 维拉斯托锡钨锂矿区石英脉型矿石中白云母的Ar-Ar坪年龄为(131.7±1.4)Ma, 显示其与外围维拉斯托铜锌矿床和拜仁达坝银铅锌矿床的成矿时代基本一致, 属同一构造-岩浆活动产物。石英斑岩中铁锂云母的Ar-Ar坪年龄为(121.9±1.3)Ma, 可能代表了最晚期的岩浆活动时限, 暗示维拉斯托矿区存在多期次岩浆-热液活动。本次研究还获得了维拉斯托矿床东南侧磨盘山岩体边部黑云母二长花岗岩锆石U-Pb年龄为(141.6±1.5)Ma(MSWD=0.75), 该年龄不仅与含矿岩体石英斑岩体的年龄一致, 也与北大山高分异杂岩体的形成年龄相近, 揭示了维拉斯托外围高分异花岗杂岩体深边部及其与地层接触带部位还有寻找锡多金属矿的巨大潜力。综合本次工作和大量前人工作的基础上, 笔者认为大兴安岭南段稀有金属矿床都形成于大陆边缘弧后伸展和软流圈上涌的构造背景, 维拉斯托锡钨锂矿化与外围脉状铅锌银铜矿化属同一岩浆-热液成矿系统, 不同金属元素在不同的矿化空间内的选择性沉淀是造成元素分带性的直接原因, 其成矿特征上可类比南美玻利维亚锡银成矿带。值得提出的是, 维拉斯托矿区岩石组合与松潘-甘孜造山带与锂矿化有关的片麻岩穹窿群类似, 锡林郭勒杂岩可能为成矿提供了部分物质来源, 对于岩浆-变形-变质-深熔作用过程及对稀有金属成矿的制约还需要进一步研究。

**关键词** 地球化学; 岩石圈伸展; 岩浆-热液成矿系统; 岩浆-变形-变质-深熔作用; 维拉斯托锡钨锂多金属矿床

**中图分类号:** P618.44; P618.67; P618.71

**文献标志码:** A

## Formation mechanism and intrinsic genetic relationship between tin-tungsten-lithium mineralization and peripheral lead-zinc-silver-copper mineralization: Exemplified by Weilasituo tin-tungsten-lithium polymetallic deposit, Inner Mongolia

ZHOU ZhenHua, GAO Xu, OUYANG HeGen, LIU Jun and ZHAO JiaQi

(MNR Key Laboratory of Metallogeny and Mineral Assessment, Institute of Mineral Resources, CAGS, Beijing 100037, China)

### Abstract

The Weilasituo Sn-polymetallic deposit is a large deposit recently discovered in southern Da Hinggan Mountains. This deposit shows a typical “upper veins+underneath mineralized granite” mineralization zoning. Besides,

\* 本文得到科技部基础资源调查专项(编号:2017FY101300、2017FY101302)、中央公益性科研院所基本业务费项目(编号:YYWF201714)和国家自然科学基金项目(编号:41772084、41302061、41820104010)的联合资助

第一作者简介 周振华,男,1981年生,副研究员,硕士生导师,从事矿床地质研究。Email: zhzhou@cags.ac.cn

收稿日期 2019-07-16; 改回日期 2019-08-16。张绮玲编辑。

the ore concentration area shows horizontal mineralization zoning: from the inner granite body outward, there exist high-T Sn-W-Mo mineralization, middle-T Cu-Zn mineralization and peripheral low-T Pb-Zn-Ag mineralization. The intrinsic genetic relationship between tin-tungsten-lithium polymetallic mineralization and peripheral vein-type lead-zinc-silver-copper mineralization, the formation mechanism and the deep geological background remain insufficiently understood. The Ar-Ar chronological study shows that the Ar-Ar plateau age of muscovite in the quartz vein-type ore in the Weilasituo tin-tungsten-lithium mining area is  $(131.7 \pm 1.4)$  Ma, which is consistent with the ore-forming ages of the peripheral copper-zinc mineralization and silver-lead-zinc mineralization and hence they belong to the same products of the tectonic-magmatic activities. The Ar-Ar plateau age of the zinnwaldite in quartz porphyry is  $(121.9 \pm 1.3)$  Ma, which may represent the latest time limit of magmatic activity, suggesting that there were multiple magmatic-hydrothermal activities in the mining area. The zircon U-Pb age of biotite monzogranite in the southeastern part of the Weilasituo deposit is  $(141.6 \pm 1.5)$  Ma (MSWD=0.75), which is not only consistent with the age of the ore-bearing rock of quartz porphyry, but also consistent with the age of the formation of the Beidashan high-differentiation complex, revealing the great tin-polymetallic prospecting potential in the peripheral area and/or in the deep part of the peripheral high-differentiation granite complex in the Weilasituo deposit. On the basis of this study and large numbers of previous research results, the authors believe that the rare metal deposits in the southern part of the Da Hinggan Mountains were formed under the tectonic background of lithospheric extensional and thinning environment. The Weilasituo tin-tungsten-lithium mineralization and peripheral vein-type lead-zinc-silver-copper mineralization belong to the same magma-hydrothermal metallogenic system, and the selective precipitation of different metal elements that occurred in different spaces is the direct reason for the elementary zonation. Moreover, its metallogenic characteristics can be analogous to those of the Bolivian tin-silver ore belt in South America. It should be pointed out that the mineral assemblages in the Weilasituo deposit are similar to those of gneiss domes associated with lithium mineralization in the Songpan-Garze orogenic belt. The Xilinguole Complex may have provided some ore-forming sources. The process of magma-deformation-metamorphism-anatexis and the constraints on rare metal mineralization deserve further study.

**Key words:** geochemistry, lithospheric extension, magma-hydrothermal metallogenic system, magma-deformation-metamorphism-anatexis, Weilasituo tin-tungsten-lithium-polymetallic deposit

锡矿床以多金属共伴生为主,单一矿种的锡矿床较少见,且常常表现出明显的矿化分带性(Meinert et al., 1997; Mao et al., 2013),中国典型的实例以广西大厂锡多金属矿田(陈毓川等,1985)、湖南柿竹园钨锡多金属矿田(毛景文等,1998;祝新友等,2016)、个旧锡矿田(毛景文等,2008)等为代表,例如,大厂矿田以龙箱盖岩体为中心形成了Zn-Cu(Sn) $\rightarrow$ Pb-Zn-Ag-Sb $\rightarrow$ Sn多金属的矿化分带;柿竹园矿田外围有东坡Pb-Zn-Ag矿和南风坳Pb-Zn-Ag矿,在千里山岩体东北接触带红旗岭脉状锡钨矿的南部外围有枞树板Pb-Zn-Ag矿,在西南部的金船塘矽卡岩型锡铋矿和才山矽卡岩型钨锡钼铋矿外围有蛇形坪和横山岭脉状Pb-Zn-Ag矿(毛景文等,2012)。国外以澳大利亚Yankee Lode钨锡多金属矿(Audébat et al., 2000; Pettke et al., 2005; Schaltegger et al., 2005)、加

拿大Mount Pleasant钨锡多金属矿(Dostal et al., 2016; Zhang et al., 2017)、西班牙Ponte Segade钨多金属矿(Canosa et al., 2012)等为代表。例如,澳大利亚Yankee Lode钨锡多金属矿围绕Mole花岗岩体从岩体向外分别发育W-Sn、Cu-Sn-As、Pb-Zn-Ag等矿化(Audébat et al., 2000)。目前,关于锡矿化与外围铅锌银矿化之间的内在成因关系还存在争论。以具有半个多世纪研究历史的大厂锡多金属矿田为例,一些学者提出大厂矿床的成矿作用至少存在2期,泥盆纪以沉积作用为主,燕山晚期经历了花岗岩浆的热液叠加改造作用,锡矿化主要与岩浆作用有关,而铅锌银矿化主要与热水沉积作用有关,锡矿化与铅锌银矿化并非同一岩浆热液体系的产物(蔡宏渊等,1983;韩发等,1997; Fan et al., 2004)。然而,大厂矿田的蚀变和矿化分带特征(陈毓川等,1985)、不同矿

化类型矿石及围岩的C-H-O同位素组成(谭泽模等,2014)、成岩成矿年代学(蔡明海等,2006;李华芹等,2008;梁婷等,2009;王新宇等,2015)、流体包裹体研究(Cai et al., 2007)、黄铁矿He-Ar同位素组成(蔡明海等,2004)等多方面证据都支持锡、钨、铜、铅、锌、锑、汞等成矿金属元素与花岗岩的演化有关(梁婷等,2014)。柿竹园矿田近接触带矽卡岩-云英岩型W-Sn-Mo-Bi矿化与远接触带脉状Pb-Zn-Ag矿化H-O-C-S-Pb多元同位素系统研究也表明,两者的成矿流体都主要为岩浆流体,矿化分带的形成与岩浆热液流体的渗透交代作用、水岩反应及岩浆流体与大气水的混合有关(吴胜华等,2016)。此外,在英国Cornwall地区钨锡多金属矿化外围的脉状Pb-Zn-Ag矿化成因上也存在沉积-热液改造(Gleeson et al., 2000)和岩浆热液成因(Müller et al., 2006)的争论,类似情况在秘鲁中部的Uchucchacua矿床同样存在(Bussell et al., 1990; Bissig et al., 2008)。

大兴安岭南段是中国北方最重要的锡多金属成矿集中区,区内已发现大-中型锡矿床4处,小型矿床和矿点30余处(王京彬等,2005)。尽管具有优越的找矿潜力,但大兴安岭南段锡矿床的成矿作用研究相对较低,极大的制约了锡矿找矿勘查的突破。最近,大兴安岭南段发现并探明维拉斯托大型锡钨锂多金属矿床(图1a),目前已查明Sn金属量8.98万吨(平均品位0.80%),Zn 1.82万吨(平均品位2.60%),WO<sub>3</sub> 1.27万吨(平均品位0.419%);初步估算Li<sub>2</sub>O矿石量5506万吨,金属量68.83万吨,平均品位1.25%(李泊洋等,2018)。矿体垂向分带性特征很明显(图1b),类似于华南钨锡矿中的“上脉下体”成矿模式(华仁民等,2015)。值得重视的是,在维拉斯托锡多金属矿东南方向不足3 km的距离范围内还依次分布有维拉斯托中型铜-锌矿床和拜仁达坝超大型银-铅-锌矿等脉状矿床(图1c)。目前已有的研究集中在单个矿床的成岩成矿时代、含矿岩体地球化学特征和流体包裹体(Liu et al., 2016; 祝新友等,2016; 翟德高等,2016; Wang et al., 2017),缺乏将锡多金属矿化与外围脉状铜锌矿化、铅锌银矿化作为一个整体进行研究,对矿床形成机制和成矿背景及不同矿化之间内在成因联系还缺乏足够的认识。本文在系统的矿床地质特征调查基础上,通过高精度年代学研究深入讨论了上述科学问题,以期促进大兴安岭地区稀有金属矿床成矿规律的研究。

## 1 区域地质背景

维拉斯托锡钨锂多金属矿位于大兴安岭南段晚古生代增生造山带,黄岗-甘珠尔庙成矿带西侧,该地区自古生代末至中生代期间经历了明显的碰撞造山、构造体制转换和板内伸展作用过程,构造-岩浆活动强烈(Sengör et al., 1996; Xiao et al., 2003)。矿区出露的地层(图1c)主要有古元古界宝音图组下段黑云斜长片麻岩、斜长角闪片麻岩、变粒岩等,即锡林郭勒杂岩;石炭系碎屑岩、碳酸盐岩主要包括古生界上石炭统本巴图组海相碎屑岩、灰岩及安山岩和阿木山组海相碎屑岩、碳酸盐岩沉积建造;上二叠统林西组粉砂质板岩、变质粉砂质泥岩,中二叠统大石寨组长石石英砂岩、粉砂质泥岩及火山凝灰岩;上侏罗统满克头鄂博组流纹岩、流纹质熔结凝灰岩,中侏罗统万宝组碳质泥岩、粉砂岩、砾岩夹煤层。第四系冲击层及风成砂土在矿区大面积出现。区域内主要的构造由贯穿全区的米生庙复背斜和断裂组成,以北东向为主,北西向断裂及近东西向断裂也较发育,构成了该区近网格状的构造格局。区域性北东向断裂构造控制着区内岩体及脉岩的分布,东西向断裂为容矿构造。

区域岩浆岩活动主要有晚石炭世和早白垩世2期。晚石炭世侵入岩主要有石英闪长岩、花岗岩、花岗闪长岩、黑云母花岗岩、黑云母二长花岗岩等,其SHRIMP锆石U-Pb年龄为298~326 Ma(刘翼飞等,2010; 王新宇等,2013),岩石具有明显的弧岩浆特征,花岗岩源区受到锡林郭勒杂岩混染作用的影响。晚石炭世石英闪长岩的w(SiO<sub>2</sub>)中等,准铝质,富Mg、Cr、Ni,(<sup>87</sup>Sr/<sup>86</sup>Sr)=0.7050~0.7076,ε<sub>Nd</sub>(t)=-0.88~1.04,具有赞岐岩的地球化学组成特征,表明其来源于俯冲流体/熔体或残余洋壳部分熔融对岩石圈地幔改造后的产物(黄丁伶等,2014)。早白垩世侵入岩主要为矿区外围东南部地区的细粒花岗岩和斑状二长花岗岩等,成岩时代在139~140 Ma(Liu et al., 2016)。区域矿产主要以锡钨锂铅锌银多金属矿化为主,维拉斯托大型锡钨锂多金属矿、维拉斯托中型脉状铜锌矿、拜仁达坝超大型脉状银铅锌矿都赋存在相近的空间范围(3 km以内),不同成矿元素组合的矿床自东向西依次产出。

## 2 矿床地质特征

维拉斯托矿床位于内蒙古克旗境内,矿区中心

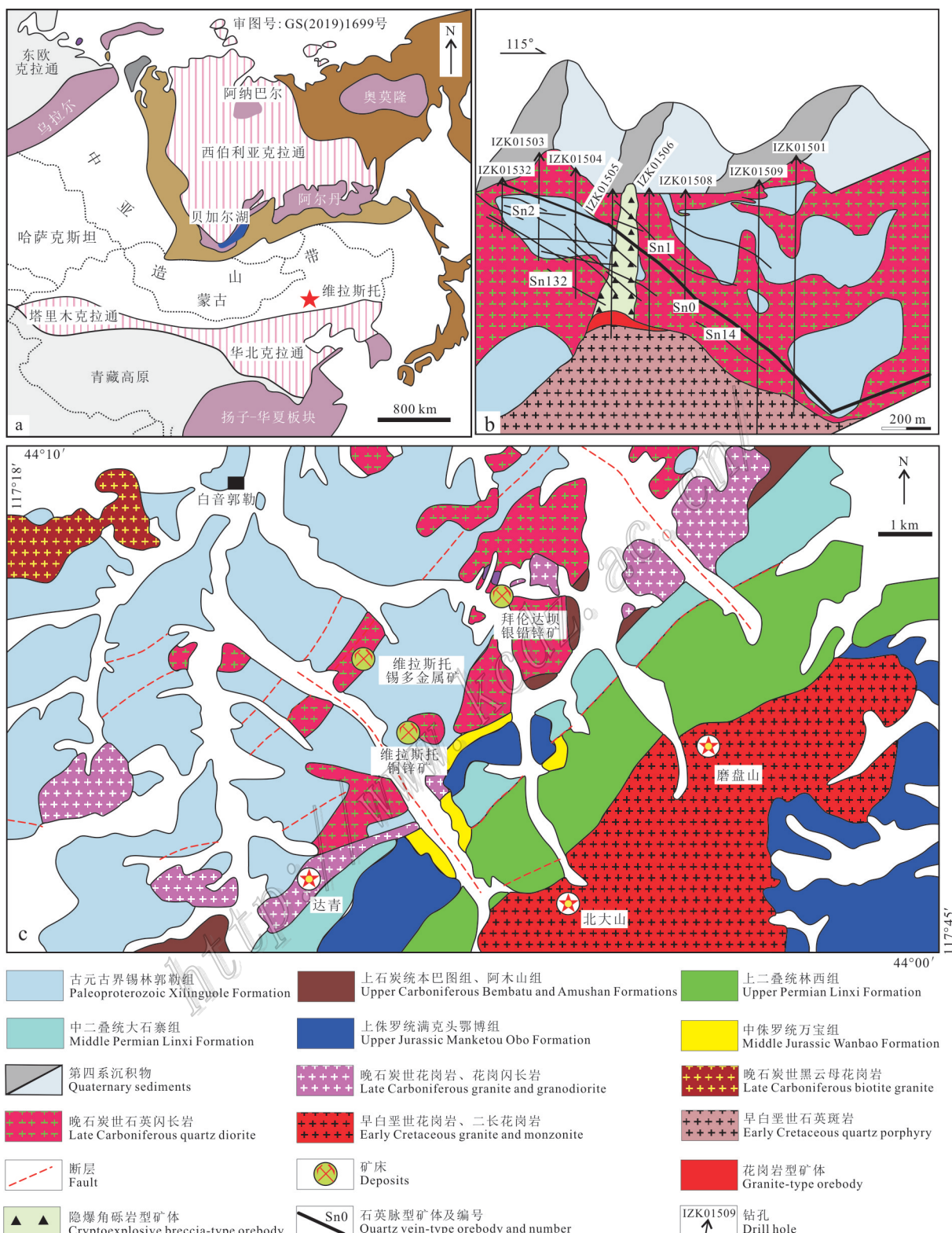


图1 中亚造山带地质简图(a, 据Jahn et al., 2000)、维拉斯托矿床主要矿体空间展布示意图(b)及拜仁达坝-维拉斯托矿田地质图(c, 据内蒙古地矿局, 2004修改)

Fig. 1 Geological map of Central Asian orogenic belt (a, after Jahn et al., 2000), sketch map of spatial distribution of main orebodies in the Weilasituo deposit(b) and geological map of the Bairendaba-Weilasituo orefield (c, modified after IMBGMR, 2004)

坐标:北纬 $44^{\circ}5'5''$ ,东经 $117^{\circ}29'53''$ 。矿区主要的容矿围岩为宝音图群黑云母斜长片麻岩、角闪斜长片麻岩(图2a),片麻状结构明显(图3a),局部出露少量石炭系石英闪长岩。矿区主要发育一组北东向断裂构造,断裂走向变化不大,沿倾向变化较大,呈波状起伏,局部发育有构造角砾岩。与成矿密切相关的岩体隐伏于锡锌矿区深部,最浅处据地表约400 m(图2b),与含钨石英脉一致。含矿岩体主要为石英斑岩,呈岩株状侵入到黑云母片麻岩和石英闪长岩中(图2c),斑晶为石英、钾长石、钠长石,岩石中

云英岩化、钠化、天河石化和碳酸盐化蚀变强烈(图3b,c)。石英斑岩体顶部附近岩相分带明显,自上而下,分别为似伟晶岩、花岗岩型矿石、矿化花岗岩和花岗岩,矿化逐渐减弱,云母、黄玉和石英含量逐渐降低,岩体内局部可见流动条带状构造,由长英质与硅质互层构成(祝新友等,2016)。

围岩蚀变以云英岩化和硅化最为强烈,此外还发育绿泥石化、绢云母化、绿帘石化、叶腊石化、高岭土化等。矿石矿物主要有锡石、闪锌矿、黄铜矿、黄铁矿,其次为黑钨矿、方铅矿、辉钼矿(图3d~n)。矿

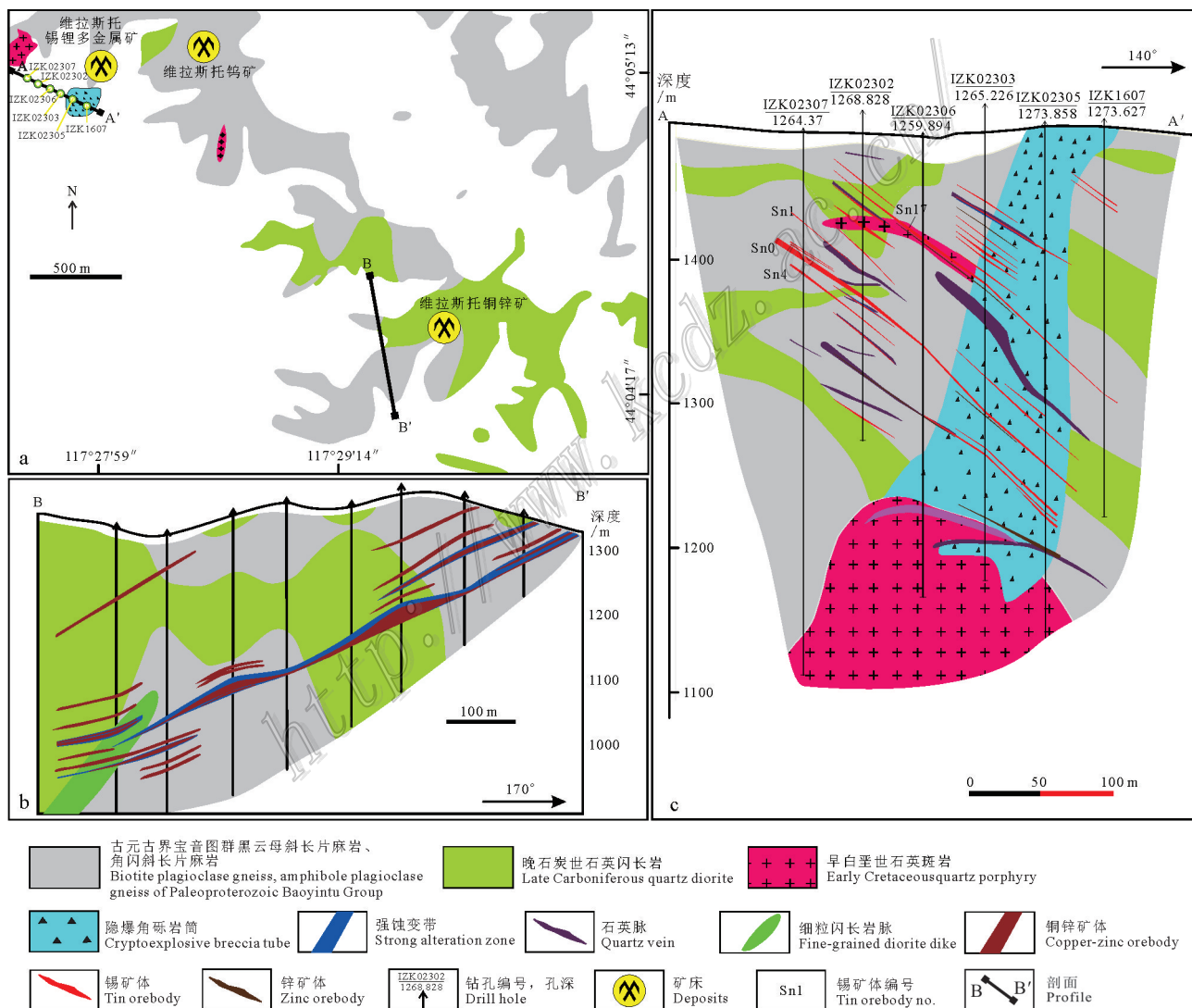


图2 维拉斯托锡钨锂多金属矿区地质图(a)、维拉斯托铜锌矿0线勘查线剖面图(b, 据内蒙古地矿局, 2004修改)及维拉斯托锡钨锂矿区I023勘探线剖面图(c, 据付旭等, 2016修改)

Fig. 2 Geological map of Weilasituo tin-tungsten-lithium-polymetallic mining area (a), geological section along No. "0" exploration line of the Weilasituo copper-zinc deposit (b, modified after IMBGMR, 2006) and geological section along No. "I023" exploration line of the Weilasituo tin-tungsten-lithium-polymetallic mining area (c, modified after Fu et al., 2016)

石结构主要有半自形粒状结构、半自形片状结构、他形粒状结构,矿石构造主要有块状、浸染状、条带状和脉状构造。脉石矿物主要有石英、方解石、萤石、黄玉、白云母、绿泥石、天河石、长石、白云石等。

维拉斯托铜锌矿区主要为平缓的顺层产出的脉状铜锌矿体(图2b),而维拉斯托锡钨锂矿区矿体垂向分带性特征很明显(图2c),类似于华南钨锡矿中的“上脉下体”成矿模式(华仁民等,2015)。深部主要是以Sn为主,伴生Zn-Rb-Nb-Ta等成矿元素的花岗岩型矿体,有经济价值的浸染状和网脉状矿化集中在石英斑岩的顶部,Sn的品位在0.3%~0.9%之间,钻孔岩芯取样结果显示:越往下矿化越弱,#200号矿体为最大矿体,标高为730~794 m,呈层状和帽状。该类型矿化中还发育有大量含矿石英细脉,沿构造裂隙贯穿;中部为以Sn为主,伴生Cu-Zn成矿元素的隐爆角砾岩筒型矿体,主要的矿石矿物为锡石、黄铜矿和闪锌矿。角砾岩型矿化与围岩之间界线不清楚,主要靠矿石的品位圈定,角砾岩筒上部发育大量鳞片状锂云母,Li、Rb等元素含量很高,具有成为独立大型稀有金属矿体的潜力;浅部为以Sn-W-Zn-Cu-Mo为成矿元素的石英大脉-网脉状矿体,是本区最主要的矿化类型和金属储量来源,矿体赋存于北东向的“S”型压扭性断裂构造中,严格受构造控制,走向上基本连续,而在倾向上有分支复合现象,局部由于矿体分支复合引起矿体品位、厚度变化较大,形态复杂。已圈定各类石英脉型矿体62条,以Sn0号矿体为矿区内最大矿体,其储量占总储量的68.27%。石英脉型矿化中矿石矿物主要有锡石、黝锡矿、黑钨矿、铁闪锌矿和斜方砷铁矿,含少量黄铜矿、黝铜矿、磁铁矿、辉钼矿、方铅矿和针硫锑铅矿。

### 3 采样位置及测试方法

#### 3.1 采样位置及描述

铁锂云母样品NW-Y-95采自维拉斯托IZK-02305钻孔622~625 m处石英斑岩中,样品为浅棕色,呈鳞片状;白云母样品WL-6-6采自6号竖井主矿体脉状铜铅锌矿石中,脉石矿物主要为石英、长石和云母,矿石矿物主要为黄铜矿、黄铁矿、闪锌矿和方铅矿等(图3l~n)。

黑云母二长花岗岩样品18WL-71采自维拉斯托矿床外围磨盘山岩体东北侧,地理坐标为E 117°31'54",N 44°0'13",样品表面风化作用明显,镜下和手

标本下观察蚀变较强(图3o~q)。岩石为灰白色,中粗粒花岗结构,块状构造。主要组成矿物为钾长石(35%),可见格子双晶;斜长石(30%)为板条状、柱状,粒度0.5~2.0 mm,可见聚片双晶结构和绢云母化蚀变;石英(30%)呈他形粒状,粒度0.2~3.0 mm,发育裂纹;黑云母含量约5%,多呈自形片状,片状,正高凸起,多色性明显,具一组完全解理,近平行消光,局部有绿泥石化蚀变;副矿物主要为磁铁矿、磷灰石、锆石等。

#### 3.2 Ar-Ar测年

云母样品经破碎、过筛、拣选,直至粒级为40~60目,然后通过砂盘淘洗、自然晾干、磁选,最后在双目镜下检查提纯云母。云母Ar-Ar同位素测年在中国地质科学院地质研究所Ar-Ar实验室完成。选用纯的矿物(纯度>99%)用超声波清洗,清洗后的样品被封进石英瓶中送核反应堆中接受中子照射。照射工作是在中国原子能科学研究院的“游泳池堆”中进行的,使用B4孔道,中子流密度约为 $2.65 \times 10^{13} \text{ n cm}^{-2}\text{s}^{-1}$ 。照射总时间为1440分钟,积分中子通量为 $2.29 \times 10^{18} \text{ n cm}^{-2}$ ;同期接受中子照射的还有用做监控样的标准样:ZBH-25黑云母标样,其标准年龄为( $132.7 \pm 1.2$ ) Ma,  $w(K)$ 为7.6%。

样品的阶段升温加热使用石墨炉,每一个阶段加热10分钟,净化20分钟。质谱分析是在多接收稀有气体质谱仪Helix MC上进行的,每个峰值均采集20组数据。所有的数据在回归到时间零点值后再进行质量歧视校正、大气氩校正、空白校正和干扰元素同位素校正。中子照射过程中所产生的干扰同位素校正系数通过分析照射过的 $\text{K}_2\text{SO}_4$ 和 $\text{CaF}_2$ 来获得,其值为: $(^{36}\text{Ar}/^{37}\text{Ar})_{\text{Ca}}=0.000\ 239\ 8$ ,  $(^{40}\text{Ar}/^{39}\text{Ar})_{\text{K}}=0.004\ 782$ ,  $(^{39}\text{Ar}/^{37}\text{Ar})_{\text{Ca}}=0.000\ 806$ 。 $^{37}\text{Ar}$ 经过放射性衰变校正; $^{40}\text{K}$ 衰变常数 $\lambda = 5.543 \times 10^{-10} \text{ a}^{-1}$ ;用ArArCALC程序计算坪年龄及正、反等时线(Anthony Koppers, v2.5.2, 2012)。坪年龄误差以 $2\sigma$ 给出。详细实验流程见有关文章(陈文等,2006;张彦等,2006)。

#### 3.3 锆石U-Pb测年

锆石在避免污染的条件下,将样品粉碎至60目以下,通过常规的重选和磁选进行初选,然后在双目镜下挑选出晶型和透明度较好的锆石。LA-MC-ICP-MS锆石U-Pb定年测试分析在中国地质科学院矿产资源研究所MC-ICP-MS实验室完成,锆石定年分析所用仪器为Finnigan Neptune型

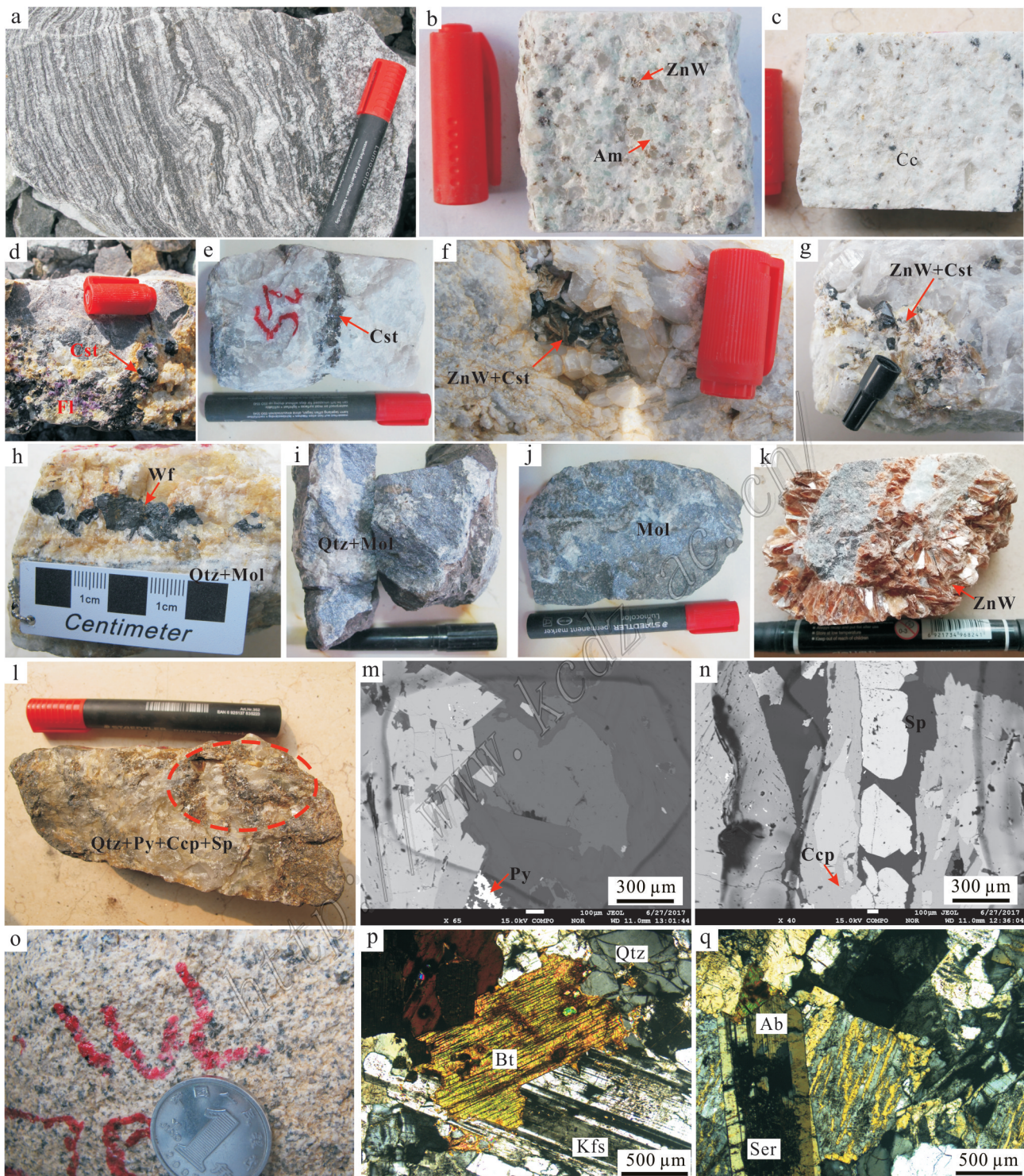


图3 维拉斯托锡钨锂多金属矿代表性岩、矿石样品照片

a. 黑云母斜长片麻岩, 片麻状结构明显; b. c. 天河石化、钠化、碳酸盐化石英斑岩; d. 石英、萤石和锡石共生组合; e. 锡石呈细脉状产出子石英脉中; f. g. 伟晶岩中粗粒自形锡石和鳞片状锂云母; h. 石英脉型黑钨矿+辉钼矿矿石; i. j. 石英脉型辉钼矿和浸染状辉钼矿矿石; k. 隐爆角砾岩筒中鳞片状锂云母; l-n. 石英脉型黄铜矿+黄铁矿+闪锌矿矿石, m, n为BSE照片; o~q. 中粗粒黑云母二长花岗岩, p, q为显微镜下照片, 黑云母解理发育; 钾长石卡巴双晶明显, 表面有泥化现象; 斜长石聚片双晶发育, 绿泥石蚀变作用较强

Am—天河石; ZnW—铁锂云母; Fl—萤石; Cst—锡石; Wf—黑钨矿; Qtz—石英; Mol—辉钼矿; Py—黄铁矿; Ccp—黄铜矿; Sp—闪锌矿;

Bt—黑云母; Kfs—钾长石; Ab—钠长石; Ser—绢云母

Fig. 3 Photographs of representative rock/ore samples of the Weilasituo tin-tungsten-lithium polymetallic deposit

a. Biotite plagioclase gneiss with obvious gneissic texture; b, c. Quartz porphyry with amazonization, sodium alteration and carbonation; d. Mineral assemblage of quartz, fluorite and cassiterite; e. cassiterite occurring in fine veins in quartz veins; f, g. Coarse-grained cassiterite and scaly zinnwaldite in pegmatite; h. Quartz vein-type wolframite+ molybdenite ore; i, j. Quartz vein type molybdenite and disseminated molybdenite ore; k. Scaly zinnwaldite in the cryptoexplosive breccia tube; l~n. Quartz vein-type chalcopyrite+pyrite+sphalerite ore, m and n are BSE photographs; o~q. Medium-coarse-grained biotite monzogranite, p and q for microscopic photographs. Biotite has fine cleavage; carlsbad twins in the potassium feldspar is obvious; plagioclase has polysynthetic twin and strong chlorite alteration  
 Am—Amazonite; ZnW—Zinnwaldite; Fl—Fluorite; Cst—Cassiterite; Wf—Wolframite; Qtz—Quartz; Mol—Molybdenite; Py—Pyrite; Ccp—Chalcopyrite; Sp—Sphalerite; Bt—Biotite; Kfs—K-feldspar; Ab—Albite; Ser—Sericite

MC-ICP-MS 及与之配套的 Newwave UP 213 激光剥蚀系统。激光剥蚀所用斑束直径为  $25\mu\text{m}$ , 频率为 10 Hz, 能量密度约为  $2.5\text{ J/cm}^2$ , 以 He 为载气。信号较小的  $^{207}\text{Pb}$ 、 $^{206}\text{Pb}$ 、 $^{204}\text{Pb}$ (+ $^{204}\text{Hg}$ )、 $^{202}\text{Hg}$  用离子计数器(multi-ion-counters)接收,  $^{208}\text{Pb}$ 、 $^{232}\text{Th}$ 、 $^{238}\text{U}$  信号用法拉第杯接收, 实现了所有目标同位素信号的同时接收并且不同质量数的峰基本上都是平坦的, 进而可以获得高精度的数据, 均匀锆石颗粒的  $^{207}\text{Pb}/^{206}\text{Pb}$ 、 $^{206}\text{Pb}/^{238}\text{U}$ 、 $^{207}\text{Pb}/^{235}\text{U}$  的测试精度( $2\sigma$ )均为 2% 左右, 对锆石标准的定年精度和准确度在 1%( $2\sigma$ )左右。LA-MC-ICP-MS 激光剥蚀采样采用单点剥蚀的方式, 数据分析前用锆石 GJ-1 进行调试仪器, 使之达到最优状态, 锆石 U-Pb 定年以锆石 GJ-1 为外标, U、Th 含量以锆石 M127( $w(\text{U})$ :  $923 \times 10^{-6}$ ;  $w(\text{Th})$ :  $439 \times 10^{-6}$ ; Th/U: 0.475; Nasdala et al., 2008)为外标进行校正。测试过程中在每测定 5~7 个样品前后重复测定 2 个锆石 GJ1 对样品进行校正, 并测量一个锆石 Plesovice, 观察仪器的状态以保证测试的精确度。数据处理采用 ICPMSDataCal 程序(Liu et al., 2009), 测量过程中绝大多数分析点的  $^{206}\text{Pb}/^{204}\text{Pb}$  大于 1000, 未进行普通铅校正,  $^{204}\text{Pb}$  由离子计数器检测,  $^{204}\text{Pb}$  含量异常高的分析点可能受包体等普通 Pb 的影响, 对  $^{204}\text{Pb}$  含量异常高的分析点在计算时剔除, 锆石年龄谐和图用 Isoplot 3.0 程序获得。详细实验测试过程可参见侯可军等(2009)。样品分析过程中, Plesovice 标样作为未知样品的分析结果为  $(337.30 \pm 2.50)\text{ Ma}$  ( $n=4, 2\sigma$ ), 对应的年龄推荐值为  $337.13 \pm 0.37(2\sigma)$  (Sláma et al., 2008), 两者在误差范围内完全一致。

## 4 测试结果

### 4.1 云母 Ar-Ar 年龄

对 2 件云母样品 NW-Y-95 和 WL-6-6 进行了 Ar-

Ar 同位素定年分析, 结果见表 1 和图 4。铁锂云母样品 NW-Y-95 经过 13 个阶段的  $^{40}\text{Ar}/^{39}\text{Ar}$  分步加热实验, 加热区间为  $700\sim1450^\circ\text{C}$ , 其中,  $820\sim1050^\circ\text{C}$  的温度阶段形成了较平坦的年龄坪, 其坪年龄为  $(121.9 \pm 1.3)\text{ Ma}$  (图 4a), 对应 90.16% 的  $^{39}\text{Ar}$  释放量。相应的反等时线年龄为  $(121.8 \pm 1.4)\text{ Ma}$  (图 4b),  $^{40}\text{Ar}/^{36}\text{Ar}$  的初始比值为  $297.8 \pm 11.2$ , 在误差范围内同大气氩比值(295.5)相近, 表明铁锂云母形成时并未捕获过剩氩。坪年龄和反等时线年龄非常一致, 坪年龄  $(121.9 \pm 1.3)\text{ Ma}$  可代表其形成时的冷却年龄。

白云母样品 WL-6-6 经过了 11 个阶段的  $^{40}\text{Ar}/^{39}\text{Ar}$  分步加热实验, 加热区间为  $700\sim1400^\circ\text{C}$ , 其中,  $940\sim1200^\circ\text{C}$  的高温阶段形成了较平坦的年龄坪, 其坪年龄为  $(131.7 \pm 1.4)\text{ Ma}$  (图 4c), 对应了 90.50% 的  $^{39}\text{Ar}$  释放量。对应的反等时线年龄为  $(132.3 \pm 1.4)\text{ Ma}$  (图 4d),  $^{40}\text{Ar}/^{36}\text{Ar}$  的初始比值为  $286.3 \pm 15.1$ , 在误差范围内同大气氩比值接近, 表明白云母形成时并未捕获过剩氩。坪年龄和反等时线年龄非常一致, 坪年龄  $(131.7 \pm 1.4)\text{ Ma}$  可代表白云母形成的冷却年龄。

### 4.2 锆石 U-Pb 年龄

黑云母二长花岗岩中锆石结晶较好, 呈典型的长柱状晶形, 具有典型的岩浆震荡环带, 指示其主体为岩浆结晶的产物。由锆石的阴极发光图像(图 5a)可以看出, 几乎所有锆石均具有清晰的单期生长的同心环带特征。

对 1 件黑云母二长花岗岩样品 18WL-71 进行了 30 个点的测试, 锆石 U-Pb 有效分析结果列于表 2, 谐和图见图 5。样品 18WL-71 的  $w(\text{U})$  和  $w(\text{Th})$  变化范围较大, 分别为  $213 \times 10^{-6}$ ~ $3695 \times 10^{-6}$  和  $74 \times 10^{-6}$ ~ $880 \times 10^{-6}$ , 部分测试点由于 U 含量或普通 Pb 含量较高, 未获得理想年龄, 在计算加权平均值时剔除。样品 18WL-71 的 14 个测点  $^{206}\text{Pb}/^{238}\text{U}$  年龄变化范围为  $135.7\sim145.6\text{ Ma}$ , Th/U 比值为  $0.23\sim0.58$ , 平均值

表1 维拉斯托矿床云母Ar-Ar同位素测年分析结果表

Table 1 Ar/Ar isotope data and apparent ages of the micas from the Weilasituo deposit

$\theta/^\circ\text{C}$	$^{36}\text{Ar}$ (fA)	$1\sigma$	$^{37}\text{Ar}$ (fA)	$1\sigma$	$^{38}\text{Ar}$ (fA)	$1\sigma$	$^{39}\text{Ar}$ (fA)	$1\sigma$	$^{40}\text{Ar}$ (fA)	$1\sigma$	$^{40}\text{Ar}^*/^{39}\text{Ar}$	$t/\text{Ma}$	$2\sigma$	$^{40}\text{Ar}$ (%)	$^{39}\text{Ar}$ (%)
NW-Y-95 铁锂云母															
700	16.1979	0.1158	0.0000	2.9855	3.0093	0.0466	8.6186	0.0329	5061.8547	2.2749	31.9465	179.2	42.51	5.44	0.12
780	23.0471	0.1504	0.0000	2.8918	4.7937	0.0350	64.4433	0.1093	8262.2676	1.3667	22.5245	128.2	7.59	17.57	0.90
820	23.3391	0.1577	0.0000	2.9906	6.9878	0.0472	224.0682	0.3766	11775.0891	2.8898	21.7671	124.0	2.33	41.42	3.13
860	13.4574	0.0992	0.0000	3.5600	11.1729	0.0763	703.3202	1.1307	18981.5828	1.1094	21.3296	121.6	0.60	79.03	9.83
890	6.5261	0.0711	0.0000	3.7186	10.2951	0.0530	742.1456	1.5095	17843.2134	20.8974	21.4394	122.2	0.65	89.17	10.37
930	4.2919	0.0468	0.0000	2.7622	9.0996	0.0540	683.5135	1.7609	15890.9826	28.3171	21.3887	121.9	0.79	92.00	9.55
970	4.5919	0.0475	0.0000	2.8741	13.7014	0.0618	1015.2712	1.6401	23248.0828	2.7887	21.5571	122.9	0.41	94.14	14.19
1010	8.3871	0.0773	0.0000	2.6861	22.2617	0.0848	1653.3555	2.9558	37701.0490	24.8978	21.2990	121.4	0.48	93.41	23.11
1050	6.9678	0.0728	0.0000	3.4486	19.3207	0.0761	1428.4353	2.3295	32416.9561	9.5414	21.2478	121.1	0.42	93.63	19.97
1100	1.3051	0.0718	0.0000	2.8892	2.8831	0.0334	226.9243	0.3737	5368.9325	2.9917	21.9553	125.0	1.11	92.80	3.17
1200	2.0487	0.0341	0.0000	3.0371	2.9535	0.0305	227.9917	0.4121	5860.8172	5.2290	23.0462	131.0	0.71	89.65	3.19
1400	9.3388	0.0687	0.0000	3.3592	3.2943	0.0396	160.2416	0.2672	6014.4878	1.9573	20.3074	116.0	1.46	54.10	2.24
1450	9.0073	0.0616	0.0000	1.4971	1.3961	0.0387	15.9009	0.0360	2831.6843	0.6522	10.6874	62.0	13.07	6.00	0.22
WL-6-6 白云母															
700	6.8076	0.0585	0.0000	25.9777	1.1958	0.0530	1.6404	0.0357	2022.4748	1.8611	6.6015	42.1	134.37	0.54	0.02
840	17.2608	0.1148	0.0000	18.4737	3.4149	0.0483	27.7234	0.0529	5494.3236	3.4029	14.1985	89.3	15.12	7.16	0.40
900	27.1068	0.1770	0.0000	22.4877	7.3969	0.0538	201.7959	0.3417	12042.4550	8.6985	19.9777	124.5	3.19	33.48	2.89
940	14.1715	0.0990	0.0000	24.1110	10.5125	0.0638	632.4838	1.0361	17510.0254	8.9897	21.0588	131.0	0.71	76.07	9.06
970	78.3925	0.5073	0.0000	24.6695	28.2507	0.0973	1089.6519	2.0966	45605.7692	54.2339	20.5897	128.1	1.82	49.19	15.61
1000	17.7749	0.1233	0.0000	17.6868	16.3091	0.0653	1024.7199	1.7673	26939.1796	22.4128	21.1588	131.6	0.67	80.48	14.68
1040	6.6314	0.0510	0.0000	20.3121	11.5467	0.0491	815.4584	1.3228	19197.3760	7.8324	21.1340	131.4	0.48	89.77	11.68
1080	9.7182	0.0737	0.0000	28.7166	28.6844	0.1009	2095.3771	3.3919	47387.5317	18.4759	21.2400	132.0	0.44	93.92	30.02
1120	2.8062	0.0292	0.0000	26.6386	4.4138	0.0307	318.2221	0.5232	7603.9335	4.0004	21.2845	132.3	0.56	89.07	4.56
1200	3.2797	0.0422	0.0000	30.4460	4.7060	0.0414	341.6726	0.5563	8232.4681	2.3964	21.2533	132.1	0.61	88.21	4.89
1400	12.2524	0.0859	0.0000	17.3347	7.6093	0.0345	432.0652	0.7137	12354.2117	7.2280	20.2089	125.9	0.84	70.68	6.19

0.37。样品测试点的Th/U均大于0.1,符合岩浆成因锆石的特征(Hoskin et al., 2000),这与锆石在CL图像上呈现的典型的岩浆震荡环带的特征是一致的。这些点均投影在谐和线上或附近,样品的 $^{206}\text{Pb}/^{238}\text{U}$ 加权平均年龄为( $141.6 \pm 1.5$ ) Ma( $2\sigma, n=14$ , MSWD=0.75)(图5b),代表了岩体的结晶年龄,与维拉斯托锡多金属矿成矿岩体石英斑岩年龄在误差范围内基本一致,均属早白垩世的产物。

## 5 讨论

### 5.1 锡-钨-锂-铅-锌-银-铜多金属成矿系统

维拉斯托锡钨锂多金属矿床的发现是大兴安岭南段近年来稀有金属找矿勘查的重要突破之一,因此也受到了国内外的广泛关注,前人对维拉斯托锡

钨锂多金属矿含矿岩体石英斑岩的LA-ICP-MS锆石U-Pb年龄测试结果为135~139 Ma(翟德高等,2016;祝新友等,2016;Liu et al., 2016),云英岩型矿石中锡石U-Pb等时线年龄为( $138 \pm 6$ ) Ma~( $135 \pm 6$ ) Ma(Wang et al., 2017),与石英脉型锡矿体中锡石U-Pb年龄( $136.0 \pm 6.1$ ) Ma(刘瑞麟等,2018a)一致。然而,维拉斯托矿区辉钼矿Re-Os年龄数据却相差较大,例如,Liu等(2016)获得辉钼矿Re-Os等时线年龄为( $135 \pm 11$ ) Ma;翟德高等(2016)对云英岩脉、石英脉、黑云母斜长片麻岩中4件辉钼矿样品的Re-Os等时线年龄测定结果为( $125.7 \pm 3.8$ ) Ma;但是郭贵娟(2016)获得的6件石英脉型辉钼矿样品的Re-Os等时线年龄却为( $116.6 \pm 1.8$ ) Ma。造成辉钼矿Re-Os年龄不一致的原因可能是样品不是同一期次或是本身样品Re/Os含量较低。最近,Gao等(2019)获得了

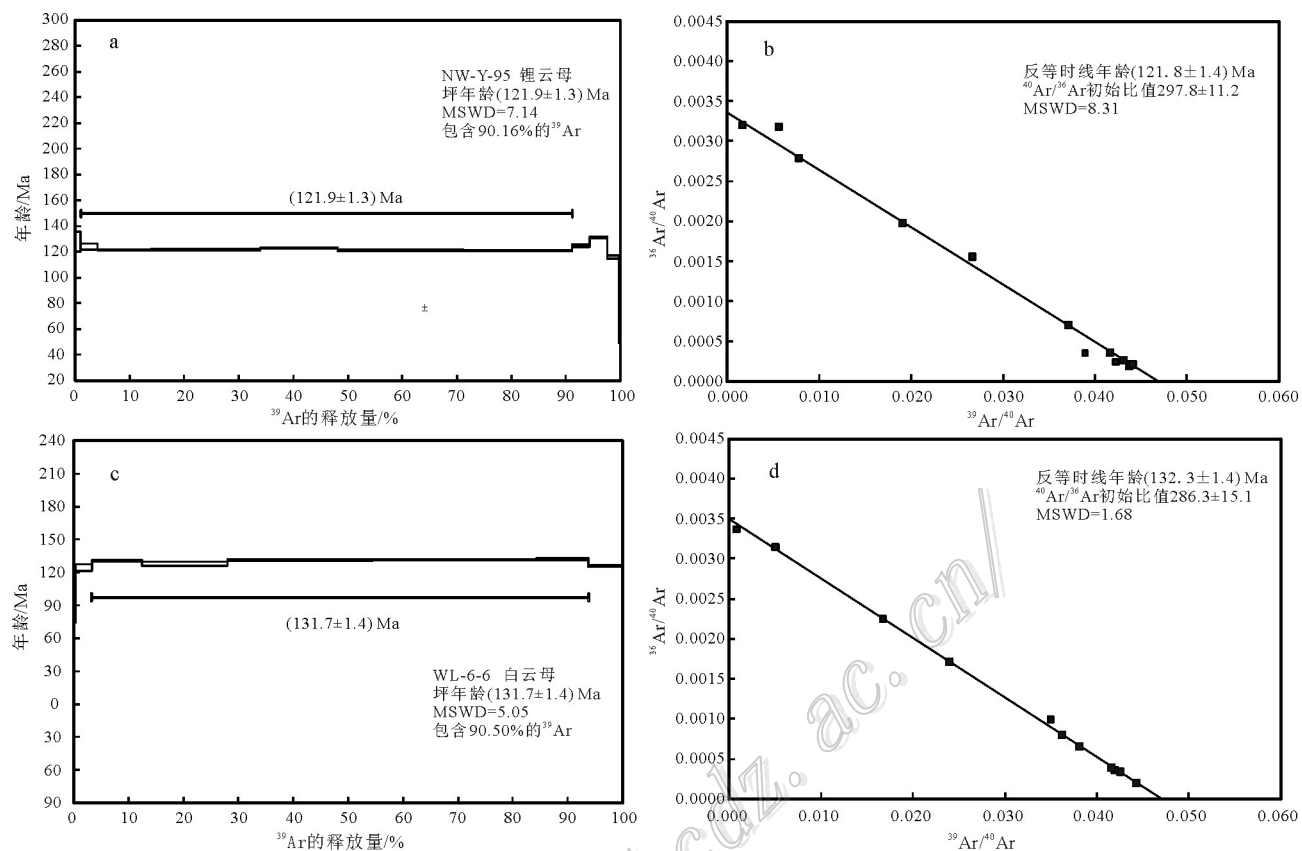


图4 维拉斯托锡钨锂多金属矿床云母 $^{40}\text{Ar}$ - $^{39}\text{Ar}$ 坪年龄(a、c)和反等时线年龄(b、d)  
Fig. 4  $^{40}\text{Ar}$ - $^{39}\text{Ar}$  spectra (a, c) and inverse isochron age (b, d) for micas from the Weilasituo deposit

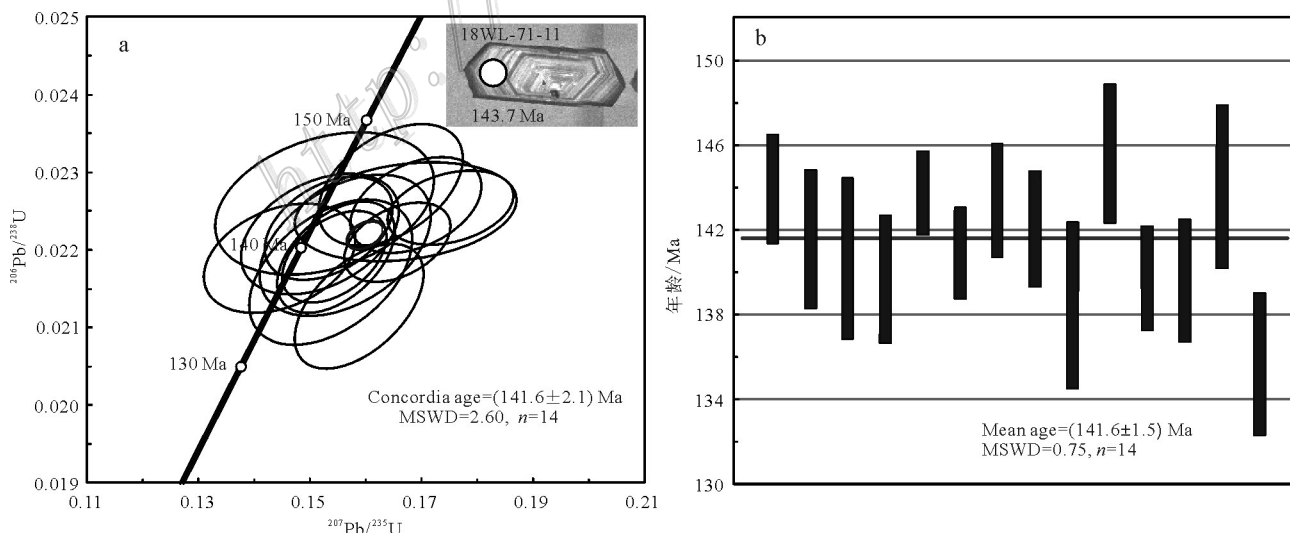


图5 维拉斯托锡钨锂多金属矿床外围黑云母二长花岗岩锆石U-Pb年龄谐和图(a)及加权平均年龄(b)  
Fig. 5 Zircon U-Pb age concordia diagram (a) and U-Pb weighted average age (b) of the biotite monzogranite from peripheral area of the Weilasituo Sn-W-Li-polymetallic deposit

表2 维拉斯托锡多金属矿外围黑云母二长花岗岩LA-ICP-MS锆石U-Pb分析数据

Table 2 LA-ICP-MS zircon U-Pb age of the biotite monzogranite in the periphery of the Weilasituo tin-polymetallic deposit

分析号	$w(B)/10^{-6}$		Th/U	年龄/Ma						比值			
	Th	U		$^{206}\text{Pb}/^{238}\text{U}$	1σ	$^{207}\text{Pb}/^{206}\text{Pb}$	1σ	$^{207}\text{Pb}/^{206}\text{Pb}$	1σ	$^{207}\text{Pb}/^{235}\text{U}$	1σ	$^{206}\text{Pb}/^{238}\text{U}$	1σ
18WL71-1	164	505	0.32	143.9	2.57	420.4	114.8	0.0552	0.0029	0.1689	0.0078	0.0226	0.0004
18WL71-4	126	390	0.32	141.6	3.26	216.7	144.4	0.0505	0.0031	0.1516	0.0093	0.0222	0.0005
18WL71-7	393	908	0.43	140.7	3.80	233.4	120.4	0.0506	0.0026	0.1562	0.0101	0.0221	0.0006
18WL71-8	231	400	0.58	139.7	3.00	287.1	111.1	0.0520	0.0025	0.1545	0.0070	0.0219	0.0005
18WL71-11	880	3695	0.24	143.7	1.98	438.9	88.9	0.0557	0.0022	0.1751	0.0075	0.0225	0.0003
18WL71-15	612	2673	0.23	140.9	2.14	372.3	85.2	0.0540	0.0020	0.1656	0.0063	0.0221	0.0003
18WL71-16	96	257	0.37	143.4	2.68	353.8	177.8	0.0536	0.0042	0.1670	0.0132	0.0225	0.0004
18WL71-19	264	664	0.40	142.0	2.75	211.2	119.4	0.0501	0.0025	0.1532	0.0076	0.0223	0.0004
18WL71-20	154	377	0.41	138.5	3.89	279.7	140.7	0.0519	0.0032	0.1536	0.0097	0.0217	0.0006
18WL71-26	164	430	0.38	145.6	3.26	388.9	133.3	0.0542	0.0032	0.1644	0.0085	0.0228	0.0005
18WL71-27	304	768	0.40	139.7	2.45	264.9	100.9	0.0515	0.0022	0.1543	0.0062	0.0219	0.0004
18WL71-28	132	394	0.34	139.6	2.91	124.2	137.0	0.0485	0.0029	0.1445	0.0090	0.0219	0.0005
18WL71-29	74	213	0.35	144.0	3.83	172.3	194.4	0.0495	0.0042	0.1526	0.0129	0.0226	0.0006
18WL71-30	706	1844	0.38	135.7	3.34	383.4	107.4	0.0543	0.0026	0.1587	0.0076	0.0213	0.0005

与黑钨矿共生的石英脉型辉钼矿的Re-Os年龄等时线年龄为( $129.0\pm4.6$ )Ma,与本次工作获得的石英脉型硫化物矿石中白云母的Ar-Ar坪年龄为( $131.7\pm1.4$ )Ma和Liu等(2016)获得的脉状矿石中白云母的Ar-Ar坪年龄( $129.5\pm0.9$ )Ma均非常一致。整体来看,维拉斯托锡多金属矿成矿时代与外围的拜仁达坝银铅锌矿和维拉斯托铜锌矿在误差范围内基本一致,后两者矿石中白云母Ar-Ar坪年龄分别为( $135.0\pm3.0$ )Ma(常勇等,2010)和( $133.4\pm0.8$ )Ma(潘晓菲等,2009),对应大兴安岭南段140~130 Ma期间与燕山晚期侵入的小岩体有关的锡铅锌铜多金属矿化高峰期(周振华等,2010)。另外,本次工作还获得石英斑岩中铁锂云母的Ar-Ar坪年龄为( $121.9\pm1.3$ )Ma,且与等时线年龄一致, $^{40}\text{Ar}/^{36}\text{Ar}$ 与大气氩比值接近,表明没有过剩氩存在,同位素体系未发生重置,代表了最晚期的岩浆活动时限,表明维拉斯托矿区可能存在多期次岩浆-热液活动,Gao等(2019)对云母等矿物的微区组成分析结果也证明了这一点。

矿化蚀变分带性在维拉斯托锡钨锂多金属矿上表现尤为明显(图1b),深部为花岗岩型和云英岩型锡钨矿化,以强烈的钠化、天河石化和云英岩化为主;上部以脉状铜锌矿化为主,矿体受“S”型压扭性断裂控制,呈脉状和透镜状,走向以近东西向为主;最顶部以隐爆角砾岩型锂云母矿化为主,角砾由黑

云母斜长片麻岩、斜长角闪片麻岩、石英闪长岩组成,胶结物主要为锂云母、石英、萤石和黄玉等。矿床东部依次分布了维拉斯托铜锌矿和维拉斯托银铅锌矿(图1c),表现出明显的成矿元素分带性,可能与成矿流体沿近东西向次级拆离带运移有关(孙爱群等,2011)。从成矿流体特征角度,维拉斯托锡钨锂多金属矿从斑岩体到云英岩,再到石英脉阶段,流体包裹体类型由以高温的熔融包裹体为主变为以熔流包裹体和含子晶三相包裹体为主,再到以中低温气液两相包裹体为主(孙雅琳等,2017;刘瑞麟等,2018b),成矿早阶段流体为高温度、高盐度( $372\sim473^\circ\text{C}$ ,  $w(\text{NaCl}_{\text{eq}})$  5.3%~50.9%),包裹体成分富含 $\text{H}_2\text{O}$ 、 $\text{CO}_2$ 和 $\text{CH}_4$ (刘瑞麟等,2018b)。维拉斯托锡钨锂多金属矿床中晚阶段成矿流体特征与维拉斯托铜锌矿床(王瑾等,2010;Ouyang et al., 2014)和拜仁达坝银铅锌矿床(王祥东等,2014;梅微等,2015)类似。闪锌矿 $\delta^{66}\text{Zn}$ 组成也清楚的记录了从维拉斯托锡钨锂多金属矿到拜仁达坝银铅锌矿东、西矿区逐渐降低的趋势(杨永强等,2010)。维拉斯托锡钨锂矿区和外围维拉斯托铜锌矿区、拜仁达坝铅锌银矿区的H-O-S-Pb同位素组成特征接近,均指示它们主要来源于深源岩浆(刘瑞麟等,2018b;江思宏等,2010;王祥东等,2014;王瑾等,2010;梅微等,2015;郭理想等,2018)。成矿流体和同位素示踪的研究反映矿化中心存在于维拉斯托锡钨锂多金属矿,一系列由于

构造隆升及岩浆侵入有关的北东向断裂构造体系成为重要的成矿、控矿构造,为含矿流体的迁移和聚集提供了有利通道和储存空间(孙爱群等,2011),锡钨锂多金属矿化与外围脉状铅锌银铜矿化属于同一岩浆-热液成矿系统。

此外,本次研究获得了维拉斯托矿床东南侧磨盘山岩体边部黑云母二长花岗岩的锆石U-Pb年龄为( $141.6\pm1.5$ )Ma,与石英斑岩体年龄一致,同时,还与北大山岩体中的细粒花岗岩、石英二长闪长岩、石英二长斑岩和二长花岗岩的时代(( $140.0\pm2.0$ )Ma~( $142.6\pm1.8$ )Ma)非常一致(管育春等,2017;刘瑞麟等,2018a)。并且,北大山岩体具有高演化的特征,岩体顶部出现富云母云英岩脉及含电气石萤石绿柱石石英脉,局部发育含黑钨矿萤石脉、含毒砂云英岩脉、含辉钼矿石英脉、含锡石电气石隐爆角砾岩等(管育春等,2017),在岩体与地层接触带部位还发育大量锡矿化带,如园林子锡铜矿、园林子北山锡多金属矿(侯跃新等,2014),表明以北大山、磨盘山为代表的早白垩世岩体与围岩接触部位具有寻找锡多金属矿的重要潜力。王京彬等(2005)提出大兴安岭南段锡多金属矿床是不同花岗岩类有关的含矿热液同位叠加成矿的结果,因此,应该重视在维拉斯托外围高分异花岗杂岩体深边部的锡矿找矿勘查工作。

## 5.2 成矿动力学背景

大兴安岭为典型的增生型造山带,经历了“三种体制(古亚洲洋、蒙古-鄂霍茨克洋、古太平洋)、两次叠合”的复杂构造演化过程(Xu et al., 2013)。从整个大兴安岭地区南段中生代岩浆演化过程看,早中生代板底垫托造成的重熔变质作用,携带幔源包体的基性岩浆上侵,早-中侏罗世基性岩墙群的扩张,一直到晚中生代大兴安岭的伸展造山,证明在100 Ma的漫长过程中,是幔隆引起的岩石圈伸展与减薄,而不是机械拉伸引起的深源岩浆上涌。而这种岩石圈伸展的深部动力可能来自地幔柱的作用(邵济安等,1998;1999a;1999b)。岩石圈减薄和软流圈物质上涌造成了强烈的壳幔相互作用和大规模成矿作用(Mao et al., 2003; 2005; Zhou et al., 2015a; 2015b)。已有的年代学结果表明,包括大兴安岭在内的整个东北地区稀有金属矿化成岩成矿的高峰期集中在130~145 Ma(王京彬等,2005;刘瑞麟等,2018a; Zhou等未发表数据),成矿时代上,从钨矿化到锡(锂)矿化,最后到铌钽铷矿化逐渐变新,也反映了成

矿演化的趋势;空间展布上,与花岗岩-伟晶岩有关的锡钨锂银铅锌铜或铌钽铷矿床主要集中在大兴安岭南段,而小兴安岭-张广才岭则主要发育花岗岩型钨矿化,是否是受蒙古-鄂霍茨克洋远程效应的影响,还是受赋矿地层的控制,还需要进一步研究。大兴安岭南段稀有金属矿床含矿岩体多为A型或高分异I型花岗岩,缺乏S型花岗岩,表明其主要形成于大陆边缘弧后伸展环境,明显不同于欧洲中部海西期大规模钨锡锂矿化成矿背景,后者主要形成于岩石圈加厚下地壳深熔作用(Gourcerol et al., 2019)。最近,Farner等(2017)的研究证实,在地壳减薄环境,残余岩浆具有高硅高分异的特征,并且主要存在于相对还原的环境,有利于稀有金属矿化的形成。

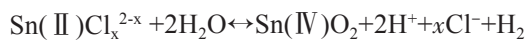
值得提出的是,包括维拉斯托锡钨锂多金属矿在内的大兴安岭南段多数稀有金属矿床都呈北东向展布于二连-贺根山缝合带和甘珠尔庙深大断裂之间(Mao et al., 2018),深大断裂带为深部幔源物质的加入提供了有利条件,氦-氩同位素证据也表明大兴安岭稀有金属矿化过程中幔源物质的参与比例较高,远大于华南地区(Gao et al., 2019)。维拉斯托锡钨锂多金属矿中辉钼矿的w(Re)较高,最高可达 $659\times10^{-6}$ ,平均 $180\times10^{-6}$ (翟德高等,2016; Gao et al., 2019),同样反映了部分深部地幔物质参与了矿床的成矿作用。幔源岩浆的底侵及软流圈对下地壳的直接加热作用引发熔融作用形成深熔花岗岩浆,并从黑云母等矿物中活化出W、Sn等成矿元素,从而引发了大规模稀有金属成矿作用(Romer et al., 2016)。

## 5.3 稀有金属超常富集机制

王京彬等(2005)认为高成熟度、富锡的锡林郭勒变质杂岩体的重熔-分异演化可能是形成大兴安岭南段锡多金属富集的主要原因。维拉斯托锡钨锂矿床中主要围岩宝音图群片麻岩即属于锡林郭勒变质杂岩体的一部分,而成矿岩体地球化学特征显示,石英斑岩为高硅、富锡(w(Sn)最高可超过 $1000\times10^{-6}$ )的过铝质花岗岩,岩石具有明显的四分组效应,Rb/Sr和K/Ba比值异常高,K/Rb、Zr/Hf、La/Nb和Eu/Eu<sup>\*</sup>比值较低,显示其分异程度较高,Sr-Nd同位素组成显示其来源于新生地壳和老基底物质的部分重熔(Wang et al., 2017; Gao et al., 2019);Gao等(2019)研究还发现维拉斯托围岩中黑云母斜长片麻岩中云母属于锂云母系列,其w(Li<sub>2</sub>O)高达4.30%~4.49%,上述特征表明围岩可能为锂矿化提供了部分成矿物质。

Romer 等(2016)强调富集的源岩和足够的热源是形成大规模锡钨矿化的必要条件,显然,维拉斯托矿床满足以上 2 个条件。但是,大兴安岭南段锡多金属矿存在成矿多样性,以最近发现的白音查干超大型锡铅锌银(锑)矿为例,该矿区并未出露锡林郭勒杂岩,而是以下二叠统大石寨组凝灰质粉砂岩、凝灰岩、安山岩、流纹岩和玄武岩为主要赋矿围岩,与成矿有关的花岗质岩石仅为中等分异程度,  $w(\text{Sn})$  并不高( $30 \times 10^{-6} \sim 90 \times 10^{-6}$ )(姚磊等, 2017),对于这类矿床的成因究竟是由于地球化学继承性(Ahlfeld, 1967; Clark et al., 1976),还是富碳和硼的泥质岩熔融作用形成的过铝质钛铁矿系列花岗岩结晶分异作用(Lehmann, 1982; 1987; Lehmann et al., 1988),还存在较大争议,需要进一步研究。饶为有趣的是,松潘-甘孜造山带大量出露的片麻岩穹窿群被认为与大规模锂矿化有关,如雅江-马尔康片麻岩穹窿群等,其核部通常由花岗质岩类岩石组成,包括石英闪长岩、黑云母二长花岗岩、二云母花岗岩、白云母钠长花岗岩等,周边为花岗片麻岩,幔部由变形的高级片岩、片麻岩和其他类型变质岩所环绕(许志琴等, 2018; 2019)。尽管结构样式与松潘-甘孜造山带的片麻岩穹窿群有所区别,但维拉斯托钨锡锂矿区同样发育类似的岩石组合,即深部钠化石英斑岩+浅部石英闪长岩+黑云母斜长片麻岩+伟晶岩+外围二长花岗岩、细粒花岗岩,对于岩浆-变形-变质-深熔作用过程及对稀有金属成矿的制约还需要进一步研究。

从地球化学属性上说,Cu、Ag、Pb、Zn 和 Sn 都属于亲铜元素,而 Mo 和 W 则属于亲石元素,它们在岩浆-热液系统中的分配行为并不一致(Greaney et al., 2017)。Li 作为最轻的元素,也是最不相容元素,岩浆演化过程中,最倾向于富集于熔浆中,因此常见于岩浆演化的最末端—花岗岩或伟晶岩(London, 2018)。在热液流体中,Sn 主要以二价的 Cl 络合物形式运移(Migdisov et al., 2005),锡石的沉淀主要是由于锡在氧化环境中由  $\text{Sn}^{2+}$  转变为  $\text{Sn}^{4+}$ ,可能的机制(Heinrich, 1990)为:



这表明任何引起酸中和或盐度降低的反应都有利于锡石的沉淀(Heinrich, 1990; Audébat et al., 2000)。维拉斯托钨锡锂矿床早期成矿流体为高温、富  $\text{CH}_4$  还原性体系,随着流体沸腾和  $\text{CO}_2$  的不断增

加及变质流体的加入,使得氧逸度急剧升高,Sn 从  $\text{Sn}^{2+}$  变为等  $\text{Sn}^{4+}$ ,从而引发锡石沉淀(Gao et al., 2019; 刘瑞麟等, 2018b)。伴随着锡石的富集沉淀的流体的不断演化,以  $\text{Cl}$  为主的含水流体不断出熔,流体温度和盐度不断降低,氧逸度不断升高,导致黑钨矿发生选择性沉淀(Wood et al., 2000; De Clercq, 2012),而银、铅、锌等也由硫氢络合物( $\text{AgHS(aq)}$ 、 $\text{Ag(HS)}^-$ 、 $\text{Ag}_2\text{S}(\text{HS})_2^{2-}$  等)转变为主要以  $\text{Cl}$  的络合物( $\text{AgClOH}^-$  等)形式运移、富集和卸载(Stefansson et al., 2003)。总体来说,维拉斯托钨锡锂多金属矿化与外围脉状银铅锌矿化是属于由高温向中低温逐渐演化、过渡的同一成矿体系,不同金属元素在不同的矿化空间内的选择性沉淀是造成元素分带性的直接原因。需要重视的是,在大兴安岭南段火山岩覆盖区陆续探明了多个银铅锌矿床,如复兴屯超大型铅锌银矿、双尖子山超大型银矿等,更为重要的是在大兴安岭多个银铅锌矿的深、边部都先后发现了锡矿化(例如边家大院、浩布高等)(Liu et al., 2018; Zhai et al., 2019),因此,与玻利维亚锡银矿带进行对比研究,深入探索大兴安岭锡银矿化的内在成因机制具有重要的科学意义。

## 6 结 论

(1) 维拉斯托钨锡锂多金属矿中石英脉型硫化物矿石中白云母的 Ar-Ar 坎年龄为  $(131.7 \pm 1.4)$  Ma,与外围脉状铜锌矿化和铅锌银矿化属同一成矿事件产物。石英斑岩中锂云母 Ar-Ar 坎年龄为  $(121.9 \pm 1.3)$  Ma,代表了最晚期的岩浆活动时限,表明维拉斯托矿区可能存在多期次岩浆-热液活动。维拉斯托矿床东南侧磨盘山岩体边部黑云母二长花岗岩的锆石 U-Pb 年龄为  $(141.6 \pm 1.5)$  Ma,该年龄与含矿岩体石英斑岩和北大山高分异花岗岩体的年龄一致,暗示维拉斯托外围高分异花岗杂岩体深边部存在较大的锡多金属找矿潜力。

(2) 矿床形成于岩石圈减薄和软流圈物质上涌背景,成矿过程中幔源物质参与比例较高,幔源岩浆的底侵及软流圈对下地壳的直接加热作用引发熔融作用形成深熔花岗质岩浆,并从黑云母等矿物中活化出 W、Sn 等成矿元素,从而引发了大规模稀有金属成矿作用。

(3) 维拉斯托矿床可类比玻利维亚锡银矿带内同类矿床,其钨锡锂矿化与外围脉状银铅锌矿化是

属于由高温向中低温逐渐演化、过渡的同一成矿体系,不同金属元素在不同的矿化空间内的选择性沉淀是造成元素分带性的直接原因。锡林郭勒变质杂岩为成矿提供了部分成矿物质,对于岩浆—变形—变质—深熔作用过程及对稀有金属成矿的制约还需要进一步研究。

**致谢** 野外地质工作期间得到了内蒙古地质勘查有限责任公司李泊洋总工、付旭、姜大伟等工程师及维拉斯托矿业公司各级领导和技术人员的大力支持。室内测试过程得到中国地质科学院矿产资源研究所侯可军副研究员的热情帮助,在此一并表示感谢。

## References

- Ahlfeld F. 1967. Metallogenetic epochs and provinces of Bolivia[J]. Minerium Deposita, 2: 291-311.
- Audétat A, Günther D and Heinrich C A. 2000. Causes for large-scale metal zonation around mineralized plutons: fluid inclusion LA-ICP-MS evidence from the Mole Granite, Australia[J]. Econ. Geol., 95: 1563-1581.
- Bissig T, Ullrich T D, Tosdal R M, Friedman R and Ebert S. 2008. The time-space distribution of Eocene to Miocene magmatism in the central Peruvian polymetallic province and its metallogenetic implications[J]. Journal of South American Earth Sciences, 26: 16-35.
- Bureau of Geology and Mineral Resources of Inner Mongolia (BGM-RIM). 2004. Detail investigation report on zinc-polymetallic deposit, west mining area of Bairendaba, Kesiketeng Banner, Inner Mongolia Autonomous Region[M]: 1-112(in Chinese).
- Bussell M A, Alpers C N, Petersen U, Shepherd T J, Bermudez C and Baxter A N. 1990. The Ag-Mn-Pb-Zn vein, replacement, and skarn deposits of Uchucchacua, Peru: Studies of structure, mineralogy, metal zoning, Sr isotopes and fluid inclusions[J]. Econ. Geol., 85: 1348-1383.
- Cai H Y and Zhang G L. 1983. A discussion of the mineralization of submarine volcanic hot spring (jet) in Dachang tin-polymetallic deposit, Guangxi[J]. Mineral Resources and Geology, 1(4): 13-21 (in Chinese).
- Cai M H, Mao J M, Liang T and Wu F X. 2004. Helium and argon isotopic components of fluid inclusions in Dachang tin-polymetallic deposit and their geological implications[J]. Mineral Deposits, 23 (2): 225-231(in Chinese with English abstracts).
- Cai M H, He L Q and Liu G Q. 2006. SHRIMP zircon U-Pb dating of the intrusive rocks in the Dachang tin-polymetallic ore field, Guangxi and their geological significance[J]. Geological Review, 52(3): 409-414(in Chinese with English abstract).
- Cai M H, Mao J W and Liang T. 2007. The origin of the Tongkeng-Changpo tin deposit, Dachang metal district, Guangxi, China: Clues from fluid inclusions and He isotope systematics[J]. Mineral Deposita, 42: 613-626.
- Canosa F, Martin-Izard A and Fuertes-Fuente M. 2012. Evolved granitic systems as a source of rare-element deposits: The Ponte Segade case (Galicia, NW Spain)[J]. Lithos, 153, 165-176.
- Chang Y and Lai Y. 2010. Study on characteristics of ore-forming fluid and chronology in the Yindu Ag-Pb-Zn polymetallic ore deposit, Inner Mongolia[J]. Peking University Journal, 46 (4): 581-593(in Chinese with English abstract).
- Chen W, Zhang Y, Jin G S and Zhang Y Q. 2006. Late Cenozoic episodic uplifting in southeastern part of the Tibetan plateau—Evidence from Ar-Ar thermochronology[J]. Acta Petrologica Sinica, 22(4): 867-872(in Chinese with English abstract).
- Chen Y C, Huang M Z, Xu J, Ai Y D, Li X M, Tang S H and Meng L K. 1985. Geological features and metallogenetic series of the Dachang cassiterite-sulfide-polymetallic[J]. Acta Prtrologica Siniaca, 3: 228-240(in Chinese with English abstract).
- Clark A H, Farrar E, Caelles J C, Haynes S J, Lortie R B, McBride S L, Quirt G S, Robertson R C R and Zentilli M. 1976. Longitudinal variations in the metallogenetic evolution of the Central Andes: A progress report[M]. Geological Association of Canada Special Paper, 14, 23-58.
- De Clercq F. 2012. Metallogenesis of Sn and W vein-type deposits in the Karagwe-Ankole belt (Rwanda)Ph. D. thesis[D]. KU Leuven. Aardk. Med, 37, 1-270.
- Dostal J and Jutras P. 2016. Upper Paleozoic mafic and intermediate volcanic rocks of the Mount Pleasant caldera associated with the Sn-W deposit in southwestern New Brunswick (Canada): Petrogenesis and metallogenetic implications[J]. Lithos, 262: 428-441.
- Fan D L, Zhang T, Ye J, Pasava J, Kribek B, Dobes P, Varrin I and Zak K. 2004. Geochemistry and origin of tin-polymetallic sulfide deposits hosted by the Devonian black shale series near Dachang, Guangxi, China[J]. Ore Geology Reviews, 24: 103-120.
- Farner M J and Lee C A. 2017. Effects of crustal thickness on magmatic differentiation in subduction zone volcanism: A global study[J]. Earth and Planetary Science Letters, 470: 96-107.
- Fu X, Huge J L T, Luo S F, Wang Y H, Zhang H Y , Qiu X F, Ding J, Zhang R J, Li W, Zhang C, Peng W G, Wang K X, Lu J H, Jia Z Y, Fu C Y, Tang L F, Zhao T Y and Wang J. 2016. Exploration report of tin-polymetallic deposit in Weilasituo mining area, Kesiketengqi Banner, Inner Mongolia Autonomous Region[R]. 1-145(in Chinese).
- Gao X, Zhou Z H, Karel Breiter, Ouyang Hegen and Liu J. 2019. Ore-formation mechanism of the Weilasituo tin-polymetallic deposit, NE China: Constraints from bulk-rock and mica chemistry, He-Ar isotopes, and Re-Os dating[J]. Ore Geology Reviews, 109: 163-183.
- Gleeson S A, Wilkinson J J, Shaw H F and Herrington R J. 2000. Post-magmatic hydrothermal circulation and the origin of base metal

- mineralization, Cornwall, UK[J]. *Journal of the Geological Society*, 157: 589-600.
- Gourcerol B, Gloaguen E, Melletton J, Tuduri J and Galiegue X. 2019. Re-assessing the European lithium resource potential—A review of hard-rock resources and metallogeny[J]. *Ore Geology Reviews*, 109: 494-519.
- Greaney A T, Rudnick R L, Helz R T, Gaschnig R M, Piccoli P M and Ash R D. 2017. The behavior of chalcophile elements during magmatic differentiation as observed in Kilauea Iki lava lake, Hawaii[J]. *Geochimica et Cosmochimica Acta*, 210: 71-96.
- Guan Y C, Yang Z F, Zhu X Y, Zou T, Cheng X Y, Tang L and Deng H H. 2017. Petrogenesis and geological significance of the Beidashan complex rock mass, Inner Mongolia[J]. *Mineral Exploration*, 8(6): 1054-1068 (in Chinese with English abstract).
- Guo L X, Liu J M, Zeng Q D, Jiang H C and Liu H T. 2018. Fluid inclusion characteristics of the Weilasituo Sn polymetallic ore deposit, Inner Mongolia, China[J]. *Earth Science Frontiers*, 25(1): 168-181 (in Chinese with English abstract).
- Guo G J. 2016. Geological characteristics and genesis of the Weilasituo tin-polymetallic deposit in Inner Mongolia[J]. Beijing: China University of Geosciences. 1-70 (in Chinese with English abstract).
- Han F, Zhao R S and Shen J Z. 1997. Geology and genesis of the Dachang tin-polymetallic deposit[M]. Beijing: Geological Publishing House. 65-157 (in Chinese with English abstract).
- Heinrich C A. 1990. The chemistry of hydrothermal tin (-tungsten) ore deposition[J]. *Econ. Geol.*, 85: 457-481.
- Hoskin P W O and Black L P. 2000. Metamorphic zircon formation by solid state recrystallization of protolith igneous zircon[J]. *Journal of Metamorphic Geology*, 18: 423-439.
- Hou K J, Li Y H and Tian Y R. 2009. In situ U-Pb zircon dating using laser ablation-multi ion counting-ICP-MS[J]. *Mineral Deposits*, 28 (4): 481-492 (in Chinese with English abstract).
- Hou Y X, Gao Q F, Wu M H and Chen Y L. 2014. Metallogenic conditions and prospecting indicators of Yuanlinzibeshan tin-polymetallic deposit in Inner Mongolia[J]. *Non-ferrous Geology in Xinjiang*, 1: 59-61 (in Chinese).
- Hua R M, Wei X L, Wang D S, Guo J S, Huang X E and Li G L. 2015. A new metallogenic model for tungsten deposit in South China's Nanling area: Up veins+underneath mineralized granite[J]. *China Tungsten Industry*, 30(1): 16-23 (in Chinese with English abstract).
- Huang D L, Zhu L T, Hou Q Y, Wang J, Liu J B, Chen Y L, Wang Z and Li D P. 2014. Geochemistry of granitoid rocks of Weilasituo deposit, Inner Mongolia and its tectonic significance[J]. *Geoscience*, 28(6): 1122-1137 (in Chinese with English abstract).
- Jahn B M, Wu F Y and Chen B. 2000. Massive granitoid generation in central Asia: Nd isotopic evidence and implication for continental growth in the Phanerozoic[J]. *Episodes*, 23: 82-92.
- Jiang S H, Nie F J, Liu Y F and Yun F. 2010. Sulfur and lead isotopic compositions of Bairendaba and Weilasituo silver-polymetallic deposits, Inner Mongolia[J]. *Mineral Deposits*, 28(1): 101-112 (in Chinese with English abstract).
- Lehmann B. 1982. Metallogeny of tin: magmatic differentiation versus geochemical heritage[J]. *Econ. Geol.*, 77: 50-59.
- Lehmann B. 1987. Tin granites, geochemical heritage, magmatic differentiation[J]. *Geol. Rundsch*, 76: 177-185.
- Lehmann B, Petersen U, Santivañez R and Winkelmann L. 1988. Distribución geoquímica de estaño boro en la secuencia Paleozoica Paleozoica de la Cordillera Real de Bolivia[M]. *Boletín de la Sociedad Geológica del Perú*, 77: 19-27.
- Li B Y, Jiang D W, Fu X, Wang L, Gao S Q, Fan Z Y, Wang K X and Huge J. 2018. Geological characteristics and prospecting significance of Weilasituo Li polymetallic deposit, Inner Mongolia[J]. *Mineral Exploration*, 9(6): 1185-1191 (in Chinese with English abstract).
- Li H Q, Wang, D H, Mei Y P, Liang T, Chen Z Y, Guo C L and Ying L J. 2008. Lithogenesis and mineralization chronology study on the Lamo zinc-copper polymetallic ore deposit in Dachang orefield, Guangxi[J]. *Acta Geologica Sinica*, 82(7): 912-920 (in Chinese with English abstracts).
- Liang T, Wang D H, Qu W J, Cai M H and Wei K L. 2009. Re-Os isotope composition and source of ore-forming material of pyrite in Tongkeng tin-polymetallic deposit, Guangxi[J]. *Journal of Earth Science and Environment*, 31(3): 230-235 (in Chinese with English abstract).
- Liang T, Wang D H, Cai M H, Fan S K, Yu Y X, Wei K L, Huang H M and Zheng Y. 2014. Metallogenic characteristics and ore-forming regularity of metallic deposits along Nandan-Hechi metallogenic belt in northwestern Guangxi[J]. *Mineral Deposits*, 33(6): 1171-1192 (in Chinese with English abstract).
- Liu L J, Zhou T F, Zhang D Y, Yuan F, Liu G X, Zhao Z C, Sun J D and Noel White. 2018. S isotopic geochemistry, zircon and cassiterite U-Pb geochronology of the Haobugao Sn polymetallic deposit, southern Great Xing'an Range, NE China[J]. *Ore Geology Reviews*, 93: 168-180.
- Liu R L, Wu G, Li T G, Chen G Z, Wu L W, Zhang P C, Zhang T, Jiang B and Liu W Y. 2018a. LA-ICP-MS cassiterite and zircon U-Pb ages of the Weilasituo tin-polymetallic deposit in the southern Great Xing'an Range and their geological significance[J]. *Earth Science Frontiers*, 25 (5): 183-201 (in Chinese with English abstract).
- Liu R L, Wu G, Cheng G Z, Li T G, Jiang B, Wu L W, Zhang P C, Zhang T and Chen Y C. 2018b. Characteristics of fluid inclusion and H-O-C-S-Pb isotopes of Weilasituo Sn-polymetallic deposit in southern Da Hinggan Mountains[J]. *Mineral Deposits*, 37(2): 199-224 (in Chinese with English abstract).
- Liu Y F, Jiang S H and Zhang Y. 2010. The SHRIMP zircon U-Pb dating and geological features of Bairendaba diorite in the Xilinhaote area, Inner Mongolia, China[J]. *Geological Bulletin of China*, 29 (5): 688-696 (in Chinese with English abstract).
- Liu Y F, Jiang S H and Bagas L. 2016. The genesis of metal zonation in the Weilasituo and Bairendaba Ag-Zn-Pb-Cu-(Sn-W) deposits in the shallow part of a porphyry Sn-W-Rb system, Inner Mongolia, China[J]. *Ore Geology Reviews*, 75: 150-173.

- Liu Y S, Gao S, Hu Z C, Gao C G, Zong K Q and Wang D B. 2009. Continental and oceanic crust recycling-induced melt-peridotite interactions in the Trans-North China Orogen: U-Pb dating, Hf isotopes and trace elements in zircons from mantle xenoliths[J]. *Journal of Petrology*, 51: 537-571.
- London D. 2018. Ore-forming processes within granitic pegmatites[J]. *Ore Geology Reviews*, 101: 349-383.
- Mao J W, Li H Y and Song X X. 1998. Geology and geochemistry of the Shizhuyuan W-Sn-Mo-Bi polymetallic deposit, Hunan[M]. Beijing: Geological Publishing House. 1-215(in Chinese with English abstract).
- Mao J W, Zhang Z H, Yu J J and Niu B G. 2003. Geodynamic settings of Mesozoic large-scale mineralisation in North China and adjacent areas-implication from the highly precise dating of ore deposits[J]. *Sciences in China (Series D)*, 46: 838-851(in Chinese).
- Mao J W, Xie G Q, Zhang Z H, Li X F, Wang Y T, Zhang C Q and Li Y F. 2005. Mesozoic large-scale metallogenic pulses in North China and corresponding geodynamic settings[J]. *Acta Petrologica Sinica*, 21(1): 169-188(in Chinese with English abstract).
- Mao J W, Cheng Y B, Guo C L, Yang Z X and Feng J R. 2008. Gejiu tin polymetallic ore-field: deposit model and discussion for several concerned[J]. *Acta Geologica Sinica*, 82(11): 1455-1467(in Chinese with English abstract).
- Mao J W, Zhang Z H and Pei R F. 2012. An introduction to mineral deposit models in China[M]. Beijing: Geological Publishing House. 81-92(in Chinese with English abstract).
- Mao J W, Cheng Y B, Chen M H and Pirajno F. 2013. Major types and time-space distribution of Mesozoic ore deposits in South China and their geodynamic settings[J]. *Mineralium Deposita*, 48: 267-294.
- Mao J W, Ouyang H G, Song S W, Santosh M, Yuan S D, Zhou Z H, Zheng W, Liu H, Cheng Y B and Chen M H. 2018. Geology and metallogeny of tungsten and tin deposits in China: An overview[J]. *Econ. Geol.*, In press.
- Mei W, Lü X B, Tang R K, Wang X D and Zhao Y. 2015. Ore-forming fluid and its evolution of Bairrendaba-Weilasituo deposits in west slope of southern Great Xing'an Range[J]. *Earth Science—Journal of China University of Geosciences*, 40(1): 145-162(in Chinese with English abstract).
- Meinert L D, Hefton K K, Mayes D and Tasiran I. 1997. Geology, zonation, and fluid evolution of the Big Gossan Cu-Au skarn deposit, Ertsberg District, Irian Jaya[J]. *Econ. Geol.*, 92: 509-534.
- Midissov A A and Williams-Jones A E. 2005. An experimental study of cassiterite solubility in HCl-bearing water vapour at temperatures up to 350°C. Implications for tin ore formation[J]. *Chemical Geology*, 217: 29-40.
- Müller A, Seltmann R, Halls C, Siebel W, Dulski, P, Jeffries T, Spratt J and Kronz A. 2006. The magmatic evolution of the Land's End pluton, Cornwall, and associated pre-enrichment of metals[J]. *Ore Geology Reviews*, 28: 329-367.
- Nasdala L, Norberg N, Schaltegger U, Schoene B, Tubrett M N and Whitehouse M J. 2008. Zircon M257: A homogeneous natural reference material for the ion microprobe U-Pb analysis of zircon[J]. *Geostandards and Geoanalytical Research*, 32: 247-265.
- Ouyang H G, Mao J W, Santosh M, Wu Y, Hou L and Wang X F. 2014. The Early Cretaceous Weilasituo Zn-Cu-Ag vein deposit in the southern Great Xing'an Range, northeast China: Fluid inclusions, H, O, S, Pb isotope geochemistry and genetic implications[J]. *Ore Geology Reviews*, 56: 503-515.
- Pan X F, Guo L J, Wang S, Xue H M, Hou Z Q, Tong Y and Li Z X. 2009. Laser microprobe Ar-Ar dating of biotite from the Weilasituo Cu-Zn polymetallic deposit in Inner Mongolia[J]. *Acta Petrologica et Mineralogica*, 28 (5): 473-479(in Chinese with English abstract).
- Pettke T, Audétat A, Schaltegger U and Heinrich C A. 2005. Magmatic-to-hydrothermal crystallization in the W-Sn mineralized Mole Granite (NSW, Australia): part II: Evolving zircon and thorite trace element chemistry[J]. *Chemical Geology*, 220: 191-213.
- Romer R L and Kröner U. 2016. Phanerozoic tin and tungsten mineralization—Tectonic controls on the distribution of enriched protoliths and heat sources for crustal melting[J]. *Gondwana Research*, 31: 60-95.
- Schaltegger U, Pettke T, Audétat A, Reusser E and Heinrich C A. 2005. Magmatic - hydrothermal crystallization in the W-Sn mineralized Mole Granite (NSW, Australia): part I: crystallization of zircon and REE-phosphates over three million years—a geochemical and U-Pb geochronological study[J]. *Chemical Geology*, 220: 215-235.
- Sengör A M C and Natal' in B A. 1996. Paleotectonics of Asia: Fragments of a synthesis[A]. In: Yin A and Harrison T M, eds. *The tectonic evolution of Asia*[M]. New York: Cambridge University Press, 486-640.
- Shao J A, Zhang L Q and Mu B L. 1998. Mesozoic tectonic-thermal evolution in the middle-south section of the Great Xing'an Range[J]. *Science in China (Series D)*: 28 (3): 193-200 (in Chinese).
- Shao J A, Zhang L Q and Mu B L. 1999a. Magmatism in the Mesozoic extending orogenic process of Da Hinggan Mts[J]. *Earth Science Frontiers (China University of Geosciences, Beijing)*, 6(4): 339-346 (in Chinese with English abstract).
- Shao J A, Han Q J, Zhang L Q and Mu B L. 1999b. Discovery of Early Mesozoic accumulative complex xenoliths in eastern Inner Mongolia[J]. *Chinese Science Bulletin*, 44(5): 478-485(in Chinese).
- Sláma J, Kosler J, Condon D J, Crowley J L, Gerdes A, Hanchar J M, Horstwood M S A, Morris G A, Nasdala L, Norberg N, Schaltegger U, Schoene B, Tubrett M N and Whitehouse M J. 2008. Plesovice zircon-A new natural reference material for U-Pb and Hf isotopic microanalysis[J]. *Chemical Geology*, 249: 1-35.
- Stefansson A and Seward T M. 2003. The hydrolysis of gold (I) in aqueous solutions to 600°C and 1500 bar[J]. *Geochimica et Cosmochimica Acta*, 67: 1677-1688.
- Sun A Q, Niu S Y, Ma B J, Nie F J, Jiang S H, Zhang J Z, Wang B D and Chen C. 2011. A comparative study of ore-forming structures

- in Bairendaba and Weilasituo silver-polymetallic deposits of Inner Mongolia[J]. Journal of Jilin University (Earth Science Edition), 41(6): 1784-1805(in Chinese with English abstract).
- Sun Y L, Xu H, Zhu X Y, Liu X and Jiang B B. 2017. Characteristics of fluid inclusion and its geological significance in the Weilasituo tin polymetallic deposit, Inner Mongolia[J]. Mineral Exploration, 8(6): 1044-1053.
- Tan Z M, Tang L F, Huang D J, Cai M H, Peng Z N, Chang J and Zhao J. 2014. Study on isotopes of carbon, hydrogen and oxygen and sources of ore-forming fluids in the Dachang tin orefield, Guangxi[J]. Mineral Exploration, 5(5): 738-743(in Chinese with English abstract).
- Wang F X, Bagas L, Jiang S H and Liu Y F. 2017. Geological, geochemical, and geochronological characteristics of Weilasituo Sn-polymetallic deposit, Inner Mongolia, China[J]. Ore Geology Reviews, 80: 1206-1229.
- Wang J, Hou Q Y, Chen Y L, Liu J B, Wang Z and Leng F R. 2010. Fluid inclusion study of the Weilasituo Cu polymetallic deposit in inner Mongolia[J]. Geoscience, 24(5): 847-855 (in Chinese with English abstract).
- Wang J B, Wang Y W and Wang L J. 2005. Tin-polymetallic metallogenetic series in the southern part of Da Hinggan Mountains, China[J]. Geology and Prospecting, 41(6): 15-20 (in Chinese with English abstract).
- Wang X D, Lü X B, Mei W, Tang R K and Li C C. 2014. Characteristics and evolution of ore-forming fluids in Bairendaba Ag-Pb-Zn polymetallic deposit, Inner Mongolia[J]. Mineral Deposits, 33(2): 406-418(in Chinese with English abstract).
- Wang X Y, Hou Q Y, Wang J, Chen Y L, Liu J B, Wang Z and Li D P. 2013. Shrimp geochronology and Hf isotope of zircon from granitoids of the Weilasituo deposit in Inner Mongolia[J]. Geoscience, 27 (1): 67-78(in Chinese with English abstract).
- Wang X Y, Huang H W, Chen N S, Huang X Q, Wu X K, Hao S and Li H M. 2015. In-situ LA-MC-ICPMS U-Pb geochronology of cassiterite from Changpo-Tongkeng tin-polymetallic deposits, Dachang orefield, Guangxi[J]. Geological Review, 61(4): 892-900 (in Chinese with English abstract).
- Wood S A and Samson I M. 2000. The hydrothermal geochemistry of tungsten in granitoid environments: I. Relative solubilities of ferberite and scheelite as a function of  $T$ ,  $P$ , pH, and  $m$  NaCl[J]. Econ. Geol., 95: 143-182.
- Wu S H, Dai P and Wang X D. 2016. C, H, O, Pb isotopic geochemistry of W polymetallic skarn greisen and Pb-Zn-Ag veins in Shizhuyuan orefield, Hunan Province[J]. Mineral Deposits, 35 (3): 633-647 (in Chinese with English abstract).
- Xiao W J, Windley B F and Hao J. 2003. Accretion leading to collision and the Permian Solonker suture, Inner Mongolia, China: Termination of the Central Asian Orogenic Belt[J]. Tectonics, 22: 1-19.
- Xu B, Zhao P, Wang Y Y, Liao W, Luo Z W, Bao Q Z and Zhou Y H. 2013. The pre-Devonian tectonic framework of Xing'an-Mongolia orogenic belt (XMOB) in North China[J]. Journal of Asian Earth Sciences, 97: 183-196.
- Xu Z Q, Wang R C, Zhao Z B and Fu X F. 2018. On the structural backgrounds of the Large-scale "Hard-rock type" lithium ore belts in China[J]. Acta Geologica Sinica, 92(6): 1091-1106(in Chinese with English abstract).
- Xu Z Q, Fu X F, Zhao Z B, Li G W, Zheng Y L and Ma Z L. 2019. Discussion on relationships of gneiss dome and metallogenic regularity of pegmatite-type lithium deposits[J]. Earth Science, 44(5): 1452-1463(in Chinese with English abstract).
- Yang Y Q, Cheng Z F, Liu H J, Shi B B, Wang J W and Lu H F. 2010. Zinc isotope study of the Bairendaba and Weilasituo polymetallic deposits, Great Xing'an Range[J]. Mineral Deposits, 33 (Supp.): 313-314(in Chinese).
- Yao L, Lü Z C, Ye T Z, Pang Z S, Jia H X, Zhang Z H, Wu Y F and Li R H. 2017. Zircon U-Pb age, geochemical and Nd-Hf isotopic characteristics of quartz porphyry in the Baiyinchagan Sn polymetallic deposit, Inner Mongolia, southern Great Xing'an Range, China[J]. Acta Petrologica Sinica, 33(10): 3183-3199(in Chinese with English abstract).
- Zhai D G, Liu J J, Li J M, Zhang M, Li B Y, Fu X, Jiang H C, Ma L J and Qi L. 2016. Geochronological study of Weilasituo porphyry type Sn deposit in Inner Mongolia and its geological significance[J]. Mineral Deposits, 35(5): 1011-1022(in Chinese with English abstract).
- Zhai D G, Liu J J, Nigel, Cook J, Wang X L, Yang Y Q, Zhang A L and Jiao Y C. 2019. Mineralogical, textural, sulfur and lead isotope constraints on the origin of Ag-Pb-Zn mineralization at Bianjiadianyu, Inner Mongolia, NE China[J]. Mineralium Deposita, 54: 47-66.
- Zhang W, Lentz D and Charnley B E. 2017. Petrogeochemical assessment of rock units and identification of alteration/mineralization indicators using portable X-ray fluorescence measurements: Applications to the Fire Tower Zone (W-Mo-Bi) and the North Zone (Sn-Zn-In), Mount Pleasant deposit, New Brunswick, Canada[J]. Journal of Geochemical Exploration, 177: 61-72.
- Zhang Y, Chen W, Chen K L and Liu X Y. 2006. Study on the Ar-Ar age spectrum of diagenetic I/S and the mechanism of  $^{39}\text{Ar}$  recoil loss—Examples from the clay minerals of  $P-T$  boundary in Changxing, Zhejiang Province[J]. Geological Review, 52(4): 556-561.
- Zhou Z H, Lü L S, Feng J R, Li C and Li T. 2010. Molybdenite Re-Os ages of Huanggang skarn Sn-Fe deposit and their geological significance, Inner Mongolia[J]. Acta Petrologica Sinica, 26(3): 667-679(in Chinese with English abstract).
- Zhou Z H, Mao J W, Liu J, Hegen Ouyang, Che H W and Ma X H. 2015a. Early Cretaceous magmatism and ore mineralization in Northeast China: Examples from Taolaituo Mo and Aobaotu Pb-Zn deposits[J]. International Geology Review, 57: 229-256.
- Zhou Z H, Mao J W, Wu X L and Hegen Ouyang. 2015b. Geochronology and geochemistry constraints of the Early Cretaceous Taibudai porphyry Cu deposit, northeast China, and its tectonic significance[J].

- Journal of Asian Earth Sciences, 103: 212-228.
- Zhu X Y, Zhang Z H, Fu X, Li B Y, Wang Y L, Jiao S T and Sun Y L. 2016. Geological and geochemical characteristics of the Weilasituo Sn-Zn deposit, Inner Mongolia[J]. Geology in China, 43(1): 188-208(in Chinese with English abstract).
- Zhuang Y, Chen W, Chen K L and Liu X Y. 2006. Study on the Ar-Ar age spectrum of diagenetic I/S and the mechanism of  $^{39}\text{Ar}$  recoil loss—Examples from the clay minerals of P-T boundary in Changxing, Zhejiang Province[J]. Geological Review, 52(4): 556-561(in Chinese with English abstract).

### 附中文参考文献

- 蔡宏渊,张国林. 1983. 试论广西大厂锡多金属矿床海底火山热泉(喷气)成矿作用[J]. 矿产地质研究院学报,1(4):13-21.
- 蔡明海,毛景文,梁婷,吴付新. 2004. 广西大厂锡多金属矿床氦、氩同位素特征及其地质意义[J]. 矿床地质,23(2):225-231.
- 蔡明海,何龙清,刘国庆. 2006. 广西大厂锡矿田侵入岩 SHRIMP 锆石 U-Pb 年龄及其意义[J]. 地质论评,52(3):409-414.
- 常勇,赖勇. 2010. 内蒙古银都 Ag-Pb-Zn 多金属矿床成矿流体特征和成矿年代学研究[J]. 北京大学学报,46(4):581-593.
- 陈文,张彦,金贵善,张岳桥. 2006. 青藏高原东南缘晚新生代幕式抬升作用的 Ar-Ar 热年代学证据[J]. 岩石学报,22(4):867-872.
- 陈毓川,黄民智,徐珏,艾永德,李祥明,唐绍华,孟令库. 1985. 大厂锡石-硫化物多金属矿带地质特征及成矿系列[J]. 地质学报,3: 228-240.
- 付旭,胡格吉乐吐,罗少飞,王永恒,张浩宇,邱显峰,丁建,张瑞军,李伟,张超,彭伟刚,王可祥,鹿建华,贾泽阳,符常渝,唐龙飞,赵太阳,王婧. 2016. 内蒙古自治区克什克腾旗维拉斯托矿区锡多金属矿勘探报告[R]. 1-145.
- 管育春,杨宗锋,祝新友,邹滔,程细音,唐雷,邓海辉. 2017. 内蒙古北大山杂岩体成因及其地质意义[J]. 矿产勘查,8(6):1054-1068.
- 郭理想,刘建明,曾庆栋,蒋胡灿,刘红涛. 2018. 内蒙古维拉斯托锡多金属矿流体包裹体特征[J]. 地学前缘,25(1):165-181.
- 郭贵娟. 2016. 内蒙古维拉斯托锡多金属矿床地质特征及成因探讨[D]. 北京:中国地质大学. 1-70.
- 韩发,赵汝松,沈建忠. 1997. 大厂锡多金属矿床地质及成因[M]. 北京:地质出版社. 65-157.
- 侯可军,李延河,田有荣. 2009. LA-MC-ICP-MS 锆石微区原位 U-Pb 定年技术[J]. 矿床地质,28(4):481-492.
- 侯跃新,高启凤,武孟豪,陈玉莲. 2014. 内蒙古园林子北山锡多金属矿成矿条件及找矿标志[J]. 新疆有色金属,1:59-61.
- 华仁民,韦星林,王定生,郭家松,黄小娥,李光来. 2015. 试论南岭钨矿“上脉下体”成矿模式[J]. 中国钨业,30(1):16-23.
- 黄丁伶,朱洛婷,侯青叶,王瑾,刘金宝,陈岳龙,王忠,李大鹏. 2014. 内蒙古维拉斯托矿区花岗岩类地球化学特征及其构造意义[J]. 现代地质,28(6):1122-1137.
- 江思宏,聂凤军,刘翼飞,云飞. 2010. 内蒙古拜仁达坝及维拉斯托锡多金属矿床的硫和铅同位素研究[J]. 矿床地质,28(1):101-112.
- 李泊洋,姜大伟,付旭,王磊,高树起,樊志勇,王可祥,胡格吉乐吐. 2018. 内蒙古维拉斯托矿区锂多金属矿床地质特征及找矿意义[J]. 矿产勘查,9(6):1185-1191.
- 李华芹,王登红,梅玉萍,梁婷,陈振宇,郭春丽,应立娟. 2008. 广西大厂拉么锌铜多金属矿床成岩成矿作用年代学研究[J]. 地质学报,82(7):912-920.
- 梁婷,王登红,屈文俊,蔡明海,韦可利. 2009. 广西铜坑锡多金属矿黄铁矿的 Re-Os 同位素组成及成矿物质来源示踪[J]. 地球科学与环境学报,31(3):230-235.
- 梁婷,王登红,蔡明海,范森葵,余阳先,韦可利,黄惠明,郑阳. 2014. 桂西北丹池成矿带主要金属矿床成矿特征及成矿规律[J]. 矿床地质,33(6):1171-1192.
- 刘瑞麟,武广,李铁刚,陈公正,武利文,章培春,张彤,江彪,刘文元. 2018a. 大兴安岭南段维拉斯托锡多金属矿床 LA-ICP-MS 锆石和锆石 U-Pb 年龄及其地质意义[J]. 地学前缘,25(5):183-201.
- 刘瑞麟,武广,陈公正,李铁刚,江彪,武利文,章培春,张彤,陈毓川. 2018b. 大兴安岭南段维拉斯托锡多金属矿床流体包裹体和同位素特征[J]. 矿床地质,37(2):199-224.
- 刘翼飞,江思宏,张义. 2010. 内蒙古锡林浩特地区拜仁达坝矿区闪长岩体锆石 SHRIMP U-Pb 定年及其地质意义[J]. 地质通报,29(5):688-696.
- 毛景文,李红艳,宋学信. 1998. 湖南柿竹园钨锡钼铋多金属矿床地质与地球化学[M]. 北京:地质出版社. 1-215.
- 毛景文,程彦博,郭春丽,杨宗喜,冯佳睿. 2008. 云南个旧锡矿田:矿床模型及若干问题讨论[J]. 地质学报,82(11):1455-1467.
- 毛景文,张作衡,裴荣富. 2012. 中国矿床模型概论[M]. 北京:地质出版社. 81-92.
- 梅微,吕新彪,唐然坤,王祥东,赵严. 2015. 大兴安岭南段西坡拜仁达坝-维拉斯托矿床成矿流体特征及其演化[J]. 地球科学(中国地质大学学报),40(1):145-162.
- 内蒙古自治区地质矿产勘查开发局. 2004. 内蒙古自治区克什克腾旗拜仁达坝西矿区锌多金属矿详查报告[M]. 1-112.
- 潘晓菲,郭利军,王硕,薛怀民,侯增谦,童英,李振祥. 2009. 内蒙古维拉斯托铜锌矿床的白云母 Ar/Ar 年龄探讨[J]. 岩石矿物学杂志,28(5):473-479.
- 邵济安,张履桥,牟保磊. 1998. 大兴安岭中南段中生代的构造热演化[J]. 中国科学(D辑),28(3):193-200.
- 邵济安,张履桥,牟保磊. 1999a. 大兴安岭中生代伸展造山过程中的岩浆作用[J]. 地学前缘,6(4):339-346.
- 邵济安,韩庆军,张履桥,牟保磊. 1999b. 内蒙古东部早中生代堆积杂岩捕虏体的发现[J]. 科学通报,44(5):478-485.
- 孙爱群,牛树银,马宝军,聂凤军,江思宏,张建珍,王宝德,陈超. 2011. 内蒙古拜仁达坝与维拉斯托很多金属矿床成矿构造对比[J]. 吉林大学学报(地球科学版),41(6):1784-1805.
- 孙雅琳,许虹,祝新友,刘新,蒋斌斌. 2017. 内蒙古维拉斯托锡多金属矿床流体包裹体特征及其地质意义[J]. 矿产勘查,8(6):

- 1044-1053.
- 谭泽模,唐龙飞,黄敦杰,蔡明海,彭振安,常江,赵京. 2014. 广西大厂矿田C、H、O同位素及成矿流体来源研究[J]. 矿产勘查, 5(5):738-743.
- 王瑾,侯青叶,陈岳龙,刘金宝,王忠,冷福荣. 2010. 内蒙古维拉斯托铜多金属矿床流体包裹体研究[J]. 现代地质, 24(5):847-855.
- 王京彬,王玉往,王莉娟. 2005. 大兴安岭南段锡多金属成矿系列[J]. 地质与勘探, 41(6):15-20.
- 王祥东,吕新彪,梅微,唐然坤,李春诚. 2014. 内蒙古拜仁达坝银铅锌多金属矿床成矿流体特征及其演化[J]. 矿床地质, 33(2): 406-418.
- 王新宇,侯青叶,王瑾,陈岳龙,刘金宝,王忠,李大鹏. 2013. 内蒙古维拉斯托矿床花岗岩类SHRIMP年代学及Hf同位素研究[J]. 现代地质, 27(1):67-78.
- 王新宇,黄宏伟,陈能松,黄锡强,吴祥珂,郝爽,李惠民. 2015. 广西大厂矿田长坡-铜坑锡多金属矿床锡石LA-MC-ICP-MS U-Pb年龄及其他地质意义[J]. 地质论评, 61(4):892-900.
- 吴胜华,戴盼,王旭东. 2016. 柿竹园钨多金属矽卡岩-云英岩与铅锌银矿脉C、H、O、Pb同位素地球化学研究[J]. 矿床地质, 35(3): 633-647.
- 许志琴,王汝成,赵中宝,付小方. 2018. 试论中国大陆“硬岩型”大型锂矿带的构造背景[J]. 地质学报, 92(6):1091-1106.
- 许志琴,付小方,赵中宝,李广伟,郑艺龙,马泽良. 2019. 片麻岩穹窿与伟晶岩型锂矿的成矿规律探讨[J]. 地球科学, 44(5):1452-1463.
- 杨永强,程泽锋,刘怀金,史冰冰,王建伟,卢鸿飞. 2010. 大兴安岭拜仁达坝及维拉斯托多金属矿床锌同位素研究[J]. 矿床地质, 33(增刊):313-314.
- 姚磊,吕志成,叶天竺,庞振山,贾宏翔,张志辉,吴云峰,李睿华. 2017. 大兴安岭南段内蒙古白音查干Sn多金属矿床石英斑岩的锆石U-Pb年龄、地球化学和Nd-Hf同位素特征及地质意义[J]. 岩石学报, 33(10):3183-3199.
- 翟德高,刘家军,李俊明,张梅,李泊洋,付旭,蒋胡灿,马立军,漆亮. 2016. 内蒙古维拉斯托斑岩型锡矿床成岩、成矿时代及其他地质意义[J]. 矿床地质, 35(5):1011-1022.
- 张彦,陈文,陈克龙,刘新宇. 2006. 成岩混层(I/S)Ar-Ar年龄谱型及<sup>39</sup>Ar核反冲丢失机理研究——以浙江长兴地区P-T界线粘土岩为例[J]. 地质论评, 52(4):556-561.
- 周振华,吕林素,冯佳睿,李超,李涛. 2010. 内蒙古黄岗夕卡岩型锡铁矿床辉钼矿Re-Os年龄及其他地质意义[J]. 岩石学报, 26(3): 667-679.
- 祝新友,张志辉,付旭,李泊洋,王艳丽,焦守涛,孙雅琳. 2016. 内蒙古赤峰维拉斯托大型锡多金属矿的地质地球化学特征[J]. 中国地质, 43(1):188-208.